CHALMERS
UNIVERSITY OF TECHNOLOGY

Estimation of driver control limitations and adaptation of intervention strategies based on crash data

Master's thesis in Systems, Control and Mechatronics

THEA LUNDMARK, SIMONE MILEVSKI

Department of Mechanics and Maritime Sciences
CHALMERS UNIVERSITY OF TECHNOLOGY
Gothenburg, Sweden 2026
www.chalmers.se

Master's thesis in Systems, Control and Mechatronics

Estimation of driver control limitations and adaptation of intervention strategies based on crash data

THEA LUNDMARK
SIMONE MILEVSKI

CHALMERS
UNIVERSITY OF TECHNOLOGY

Department of Mechanics and Maritime Sciences
Vehicle Safety
Chalmers University of Technology
Gothenburg, Sweden 2026

Estimation of driver control limitations and adaptation
of intervention strategies based on crash data
THEA LUNDMARK
SIMONE MILEVSKI

© THEA LUNDMARK, SIMONE MILEVSKI, 2026.

Supervisor: Thomas Streubel, Safety Center, Volvo Car Corporation
Supervisor: Linda Pipkorn, Department of Mechanical Engineering
Examiner: Jonas Bärgman, Department of Mechanical Engineering

Master's Thesis 2026
Department of Mechanics and Maritime Sciences
Vehicle Safety
Chalmers University of Technology
SE-412 96 Gothenburg
Sweden
Telephone +46 31 772 1000

Cover: Visualizes the use of ADAS in traffic.

Typeset in LaTeX
Gothenburg, Sweden 2026

Estimation of driver control limitations and adaptation of intervention strategies based on crash data
Master's thesis in Systems, Control and Mechatronics
THEA LUNDMARK
SIMONE MILEVSKI
Department of Mechanics and Maritime Sciences
Vehicle Safety
Chalmers University of Technology

Abstract

Sweden's Vision Zero initiative aims to eliminate fatalities and serious injuries in road transportation. A key component is the development of Advanced Driver Assistance Systems (ADAS), supporting drivers in crash-imminent situations. However, determining the optimal timing and magnitude of system interventions remains challenging, as interventions should support rather than conflict with the driver's intended maneuver. One proposed approach is to define driver control limitations, such as maximum braking and steering inputs, and use these limitations to support ADAS intervention design.

This thesis analyzes real-world crash data to evaluate driver control limitations using four metrics: Steering Wheel Angle (SWA), Steering Wheel Angle Velocity (SWAV), Driver Deceleration Request (DDR), and Actual Time-to-Collision (ATTC). Actual vehicle deceleration was also considered relevant to distinguish between driver-related braking demand and the resulting vehicle response. The metrics were examined across varying driving contexts, including vehicle speeds, vehicle actions, crash types, road and lighting conditions, and ADAS activation.

The results showed that SWA varied slightly with maneuver type, while SWAV remained more consistent and may represent a more stable upper limit of steering behavior. Most drivers reached maximum deceleration request; however, the ATTC results showed that braking was often initiated too late to prevent a collision. DDR alone was insufficient in low-friction conditions, highlighting the importance of considering actual vehicle deceleration. ADAS activation generally had limited influence.

Simulation results indicate that refined steering thresholds may allow drivers to avoid obstacles where current ADAS would intervene prematurely. These findings support incorporating driver control limitations into future ADAS development.

Keywords: Driver behavior, control limits, crash data analysis, statistical analysis.

Acknowledgements

This report presents the outcome of our master's thesis project carried out at the Department of Mechanical Engineering at Chalmers University of Technology during the spring of 2026.

First, we would like to thank our supervisor at Volvo Cars Corporation, Thomas Streubel, for his guidance, engagement, and valuable input during the project. His knowledge within vehicle safety, active safety systems, and driver behavior has been highly valuable for the development of this work.

We would also like to thank our academic supervisor, Linda Pipkorn, and our examiner, Jonas Bärgman, at Chalmers University of Technology, for their support, constructive feedback, and guidance throughout the thesis process.

In addition, we are grateful to the Volvo Cars Safety Center for providing access to the crash database and for sharing important knowledge regarding the data, annotations, and interpretation of real-world crash scenarios. This support has been essential for carrying out the analysis presented in this thesis.

Thea Lundmark, Simone Milevski, Gothenburg, June 2026

List of Acronyms

Below is the list of acronyms that have been used throughout this thesis listed in alphabetical order:

AASHTO	American Association of State Highway and Transportation Officials
ABS	Anti-lock Braking System
ACC	Adaptive Cruise Control
ADAS	Advanced Driver Assistance System
AEB	Autonomous Emergency Braking
ANOVA	Analysis of Variance
ATTC	Actual Time-to-Collision
CI	Confidence Interval
CMbB	Collision Mitigation by Braking
DDR	Driver Deceleration Request
eLKA	Emergency Lane Keeping Assist
FARS	Fatality Analysis Reporting System
FCW	Forward Collision Warning
GES	General Estimates System
GDPR	General Data Protection Regulation
ITE	Institution of Transportation Engineers
KDE	Kernel Density Estimation
LKA	Lane Keeping Assist
LTAP	Left-turn-across-path
PRT	Perception Response Time
RQ	Research Question
ROR	Run-off-road
SAE	Society of Automotive Engineers
SCP	Straight crossing path
SWA	Steering Wheel Angle
SWAV	Steering Wheel Angle Velocity
TTC	Time-to-Collision
VRU	Vulnerable Road User

Contents

List of Figures

List of Tables

1
Introduction

Sweden's Vision Zero initiative represents a fundamental shift in road safety policy, aiming to eliminate fatalities and serious injuries in road transportation (Trafikverket, 2022, 2024). Introduced by the Swedish government in 1997, the initiative sets ambitious targets, including limiting road traffic fatalities to 133 and severe injuries to 3,100 by 2030. Achieving these goals requires designing a road transport system that tolerates human error without leading to serious or fatal outcomes (Bellin et al., 2012).

Within the Vision Zero framework, road safety is understood as a system-level responsibility in which human errors are anticipated and mitigated through the design of the road transport system as a whole (Elvebakk, 2007). In this context, vehicle-level technologies, such as automated driving functions and driver-support functions, can contribute to road safety by assisting the driver and enhancing the vehicle's ability to respond safely in critical situations (Bachute & Subhedar, 2021).

Advanced Driver Assistance Systems (ADAS) include a broad range of vehicle functions for active safety and driver support, with varying documented safety benefits, and are therefore relevant across different driving scenarios (European Commission, 2021; Winner et al., 2016). These functions can be conceptualized along dimensions such as urgency and degree of control, ranging from comfort functions designed to support the driver and enhance driving comfort, to active safety functions intended to intervene in safety-critical situations (de Winkel & Christoph, 2025).

ADAS functions such as Adaptive Cruise Control (ACC) and Lane Keeping Assistance (LKA) are often associated with comfort functions, as they aim to reduce driver workload during normal driving conditions (DeGuzman and Donmez, 2021). Still, these comfort functions offer safety-related benefits in specific conflict scenarios, for example, by reducing rear-end collisions with ACC or reducing the number of single-vehicle lane departures with LKA (Alkim et al., 2007; Costa, 2019).

In case of an imminent threat, active safety functions such as Autonomous Emergency Braking (AEB) and Emergency Lane Keeping Assist (eLKA) (de Winkel & Christoph, 2025) can intervene. These functions are designed to intervene in critical situations with the aim of preventing or mitigating collisions and unintended lane departures, respectively (Deng & Zahabi, 2025).

These safety functions are typically triggered based on threshold values of minimum

time-to-collision (TTC) with a lead vehicle. However, such activation strategies may conflict with the driver's intentions in crash-imminent situations, potentially leading to irritation, confusion, and discomfort. Consequently, there is a need to better anticipate driver behavior in these scenarios and to adapt ADAS accordingly (Gao et al., 2024).

Accurately predicting driver behavior remains a major challenge in the development of effective active safety functions (Bhattacharyya et al., 2025). This challenge arises from the fact that driver responses in critical situations have been shown to vary significantly among individuals (Wu & Lin, 2019). Such inter-individual variability makes it difficult to reliably estimate driver responses in critical situations. One consequence of this uncertainty is that drivers may adopt different avoidance strategies in identical situations. For example, one driver may prefer steering while another may choose braking, potentially leading the vehicle to initiate a maneuver that conflicts with the driver's intention. In addition, drivers may exhibit different levels of maneuver intensity under similar conditions (Papazikou et al., 2021). Consequently, determining the optimal moment for system intervention, particularly in situations where the driver is unlikely to successfully avoid the collision without assistance from the system, remains a key challenge.

The effectiveness of collision avoidance by human drivers depends not only on their ability to perceive and react, but also on applying appropriate control inputs (X. Wang et al., 2016). The magnitude and timing of these driver inputs, such as steering and braking, play a crucial role in collision avoidance (Frydrýn et al., 2025; Markkula, 2014). In some situations, these inputs may be insufficient to fully utilize the vehicle's dynamic capabilities, thereby limiting the driver's ability to mitigate or avoid collisions (X. Wang et al., 2016).

To address the challenge of determining appropriate intervention timing for active safety functions, this thesis investigates which metrics can be used to evaluate driver control limitations and subsequently focuses on identifying these limitations under different driving conditions. By establishing these limitations, they may be used as guidelines for future development of ADAS. In this thesis, driver control limitations are defined as the maximum braking and steering abilities of a driver. These limitations include both the magnitude of the input and the timing of the intervention. Incorporating driver control limitations into the parameterization of active safety functions can improve the alignment between system behavior and human performance, thereby enhancing the effectiveness of interventions and contributing to collision reduction (Markkula, 2015).

1.1 Background

This section presents an overview of driver behavior and the variables used to characterize steering and braking actions. It further introduces different crash types and vehicle actions as well as how road surface conditions and tire-road friction constrain the interaction between driver inputs and vehicle response. Finally, this

section presents how lighting conditions can affect drivers and the probability of collisions.

1.1.1 Steering behavior

To better understand driver control limitations, steering behavior has been shown to provide valuable insights into driver state and intentions. Previous research demonstrates that analysis of steering wheel data can be used to predict lane changes (Planek et al., 2014), detect driver fatigue (Li et al., 2022), and support automated steering interventions (Frydrýn et al., 2025). These applications highlight the importance of steering input not only as a control action of the car, but also as an indicator of driver behavior and underlying driver state.

Steering plays a critical role in accident avoidance, particularly in situations where braking alone is insufficient to prevent a collision. Previous studies have shown that most drivers do not steer sufficiently when faced with the risk of rear-end collisions, even though approximately 50.0% of such critical situations could potentially have been avoided through adequate steering input (Harinath et al., 2020). Furthermore, collision avoidance based solely on braking requires earlier intervention compared to combined steering and braking maneuvers. Notably, collision avoidance may remain possible through steering even when it is too late to stop the vehicle by braking alone (Blommer et al., 2017). These findings suggest that steering is not merely complementary to braking, but may in certain scenarios represent a decisive avoidance mechanism.

To quantify steering behavior, key variables include the steering wheel angle (SWA) [°, rad] and steering wheel angle velocity (SWAV) [°/s, rad/s] as these variables directly influence vehicle trajectory and stability during evasive maneuvers (Frydrýn et al., 2025).

1.1.1.1 Steering wheel angle

The maximum SWA reached by a driver varies significantly depending on whether the maneuver is a routine overtaking maneuver or an emergency evasion (Breuer, 2017; Planek et al., 2014). In this thesis, SWA refers to the angular rotation of the steering wheel relative to its neutral position when driving straight ahead. For example, in a standard overtaking maneuver, a study with 51 participants in a driving simulator reported maximum SWA values of approximately 40.0° (Planek et al., 2014).

In contrast, the "Moose-test", which represents emergency evasive maneuvers conducted without braking on a test track, has been reported to involve substantially larger steering inputs (Breuer, 2017). At a vehicle dynamics workshop where a new vehicle was presented to the press, more than 400 motor journalists conducted the moose test using a vehicle equipped with data acquisition systems to capture driver inputs. The same test protocol was also conducted by a group of 30 non-professional drivers (referred to as normal drivers). At speeds between 60.0 and

80.0 km/h, the mean maximum SWA for 399 motor journalists was approximately 170°, while slightly lower values were observed for the normal drivers. Furthermore, the same study provided data from real road traffic for the 30 normal drivers, where maximum SWA remained considerably lower, reaching values around 80.0°. This difference in SWA was subsequently discussed as being attributable to the real-world traffic context, where braking, either alone or in combination with steering, can be applied. Previous studies had shown that braking, or braking combined with steering, represents the most common driver response in critical situations, which may reduce the magnitude of steering inputs compared to test-track maneuvers.

Another study tested various maneuvers around a three-meter-long obstacle across different speeds and maneuver categories on a test track, using sharp maneuvers to represent critical crash-avoidance situations (Frydrýn et al., 2025). For sharp maneuvers at 50.0 km/h, the average steering wheel angle at maximum SWAV was 100.0°, with an interval of 90.0–110.0°. At 70.0 km/h, the average steering wheel angle at maximum SWAV was 83.0°, with an observed interval of 67.5–90.0°. At 90.0 km/h, the average steering wheel angle at maximum SWAV was 73.0°, with an interval of 67.5–87.0°.

While these studies report the steering wheel angle, it is important to highlight that the steering ratio, which describes the relationship between the steering wheel angle and the road wheel angle, is vehicle-specific. The ratio differs between lighter and heavier vehicle types and varies between approximately 12:1 and 28:1 (Heisler, 2002). Vehicle weight is therefore one factor contributing to this variation, as heavier vehicles often require a higher ratio to reduce the physical effort needed to steer. This means that the same steering wheel angle can correspond to different actual wheel angles depending on the vehicle. For example, a steering ratio of 12:1 means that a 120° steering wheel rotation corresponds to approximately 10° of road wheel rotation, whereas a ratio of 24:1 would correspond to approximately 5°.

1.1.1.2 Steering wheel angle velocity

The previously mentioned "Moose-test" study also showed that the maximum SWA and maximum SWAV are correlated ($r^2 = 0.670$) (Breuer, 2017). This indicates that maneuvers involving larger steering wheel angles generally also involve higher steering wheel angle velocities.

In one study, drivers performed evasive maneuvers around a three-meter-long obstacle at three vehicle speeds and within three predefined maneuver categories: mild, moderate, and sharp, where the sharp maneuver represented a critical evasive maneuver (Frydrýn et al., 2025). The study found that vehicle speed had a comparatively small effect on the average SWAV, whereas the maneuver category had a larger effect. Between the lowest speed (50.0 km/h) and the highest speed (90.0 km/h), the average SWAV differed by at most approximately 19.0°/s within a single maneuver category. In contrast, at a constant speed of 90.0 km/h, the average SWAV increased from 42.0°/s for mild maneuvers, to 93.0°/s for moderate maneuvers, and to 183.0°/s for sharp maneuvers. The highest average maximum SWAV

reached for the sharp maneuver was also observed for the intermediate velocity (70.0 km/h) at 372°/s. These findings suggest that the predefined maneuver category had a stronger influence on steering angle velocity than vehicle speed. Conversely, other studies have shown that the maximum SWAV decreases significantly as vehicle speed increases (Breuer, 2017).

However, the maximum SWAV does not only vary among different maneuvers but also in the literature. Based on empirical observations, Blundell and Harty (2015) proposed three driving regimes, partly characterized by different ranges of handwheel rate. Considering only the handwheel-rate component of this classification, the regimes are:

- Normal driving: $0 - 400°/s$
- Spirited driving: $400 - 700°/s$
- Accident avoidance: $700 - 1200°/s$

These ranges are therefore used as empirical reference values for interpreting SWAV levels, rather than as fixed driver-specific limits.

The "Moose-test" also evaluated SWAV and reported maximum values ranging from 292 to 1335°/s, with an average maximum value of 746°/s (Breuer, 2017). This large variation suggests that steering responses differed considerably between participants and test runs. The study indicates that performance in the maneuver was strongly influenced by how each driver steered, including differences in skill level and motivation. Therefore, previously reported SWAV ranges should be interpreted as empirical reference values rather than fixed limits that are independent of the driver.

1.1.2 Braking behavior

In addition to steering, braking behavior is a crucial component in accident avoidance, as both the magnitude and the timing of braking determine whether a collision can be prevented (Durrani et al., 2021). Previous research also suggests that higher situational urgency is associated with stronger braking responses, including higher maximum brake pedal pressure and peak deceleration (X. Wang et al., 2016). One way to evaluate braking magnitude is by analyzing the brake pedal force [N] applied by the driver (Garrosa et al., 2021). This variable can be analyzed in combination with the vehicle's actual deceleration, measured in $[m/s^2]$ (Gillespie, 2021). By evaluating both variables together, the relationship between braking demand and the actual response of the vehicle can be investigated.

Braking behavior, including brake pedal force and the time required to reach maximum deceleration, is influenced by driving conditions and driver-related factors such as demographics, driving profession, and driving history (Pawar et al., 2020). In rear-end scenarios, deceleration has also been observed to be lower when there is no directly preceding vehicle, or when the preceding vehicle is traveling faster than the ego vehicle, meaning that the distance between the vehicles is increasing (Varotto et al., 2021).

In this thesis, the requested deceleration is used as an indirect indicator of driver-related braking demand, as brake pedal force and internal brake system signals are not available in the dataset. However, the available driver deceleration request may include brake system gain, meaning that it cannot be interpreted as a pure measure of brake pedal input. The resulting vehicle deceleration is therefore also analyzed to describe the physical vehicle response.

1.1.2.1 Driver deceleration request

The driver deceleration request (DDR) represents a driver-related braking demand rather than the achieved vehicle response. However, as described above, the signal may include brake system gain and should therefore not be interpreted as a pure measure of brake pedal input. This distinction is important, as the requested deceleration may differ from the actual vehicle deceleration (Aleksendrić et al., 2012).

One study, conducted on a closed test track, investigated driver braking performance when participants were unexpectedly confronted with an obstacle spanning the full width of the roadway, requiring an immediate braking response (Fitch et al., 2010). Of the 64 participants, only eleven were able to bring the vehicle to a complete stop. To estimate maximum driver control limits, the analysis therefore focused on these eleven drivers. For this subset, a mean deceleration of 0.48 g ($\approx$ 4.71 m/s^2) was observed, with a maximum deceleration of 0.61 g ($\approx$ 5.98 m/s^2). In addition, the study reported that the mean maximum brake pedal force that drivers were capable of exerting was 196 lbs ($\approx$ 88.9 kg), while the mean maximum force applied during the braking maneuver was only 36 lbs ($\approx$ 16.3 kg). This finding indicates that, on average, drivers utilized only about 18.4% of their available braking capacity.

1.1.2.2 Vehicle deceleration

When examining the vehicle's actual deceleration, values reported in the literature vary widely depending on the driving context, as discussed in more detail in Section 1.1.4. However, some driving databases do not include detailed contextual information, in which case a general maximum vehicle deceleration can be obtained. In the following, several studies are reviewed to provide an overview of the maximum vehicle's actual deceleration observed in crash-imminent situations.

One study based on the UDRIVE database examined driver behavior on motorways when traffic congestion suddenly appeared (Varotto et al., 2021). In that study, only events in which vehicle deceleration reached at least 0.5 m/s^2 were included, since lower values were considered to represent normal driving with minor corrective braking rather than intentional braking events (Deligianni et al., 2017). This threshold will therefore be used in this report to distinguish more pronounced braking events from minor corrective speed adjustments. In addition, the study only considered events with an initial speed greater than 50 km/h and a speed reduction exceeding

5 km/h. Based on these inclusion criteria, 1,060 deceleration events were identified and used for further analysis. The maximum deceleration observed was 8.76 m/s^2, while the mean deceleration was substantially lower, at 1.72 m/s^2.

In contrast, a study based on SHRP2 Naturalistic Driving Study (NDS) data reported slightly higher values, where the maximum deceleration reached was $1.15\,g$ ($\approx 11.3 m/s^2$) for near-crashes (Papazikou et al., 2021). The authors further suggested a threshold within the range of $0.300 - 0.600\,g$ ($\approx 2.94 - 5.89 m/s^2$) as an indicator of braking associated with safety-critical events.

Although conducted on a test track under dry asphalt conditions, another study examining drivers' collision avoidance behavior reported a similar maximum longitudinal deceleration of 1.15g, in agreement with Papazikou et al. (2021) (Mazzae et al., 2003).

The maximum vehicle deceleration has also been shown to vary depending on vehicle type. One study based on the Insurance Institute for Highway Safety's (IIHS's) Front Crash Prevention (FCP) evaluations investigated braking performance across vehicles with different safety ratings (Kidd et al., 2023). The analysis included a subset of the database comprising 3,231 FCP tests conducted at speeds of 20 km/h and 40 km/h. The results indicated that superior-rated vehicles demonstrated higher braking performance (e.g., -9.27 m/s^2 at 40 km/h), whereas basic/advanced-rated vehicles exhibited lower braking performance (e.g., -7.19 m/s^2 at 40 km/h).

Since the maximum deceleration levels reported in the literature are relatively consistent, they provide useful reference values for identifying unusually high vehicle deceleration levels in the analyzed data. Using this guideline, together with the defined thresholds from Deligianni et al., 2017 and Mazzae et al., 2003, the vehicle's actual deceleration can be analyzed within a more precise analytical context.

1.1.2.3 Timing of braking

While braking magnitude determines the physical capability to avoid a collision, the timing of brake initiation is equally critical. The initiation of braking is commonly described using Perception Response Time (PRT), defined as the time required to identify, interpret, and decide upon a hazard, as well as to initiate brake application (Xue et al., 2018).

Determining when to start measuring PRT is not straightforward, as it is defined to begin when the driver first detects a hazard. The nature of the hazard may vary across scenarios. For example, PRT may be initiated when the brake lights of a lead vehicle become visible or when an unexpected object enters the driving path (National Academies of Sciences, Engineering, and Medicine, 2024).

Determining the end of the PRT interval may appear simpler, however, the point in time at which drivers initiate their response can be interpreted in several ways. Examples of possible definitions for the end of PRT include the moment the driver

makes contact with the brake pedal, the onset of brake light activation, or the time at which a specified deceleration threshold is reached (Dinakar and Muttart, 2019).

Furthermore, numerous studies have investigated how PRT is influenced by various factors. For example, one simulation study examined the effect of situational urgency, or criticality of the situation, on PRT by varying headway and lead vehicle deceleration during a car-following scenario (X. Wang et al., 2016). The analysis incorporated measurements of PRT, throttle release times, throttle to brake transition times, brake delays maximum brake pedal force and peak deceleration to assess the influence of situational urgency on PRT. The results showed that driver response times vary with situational urgency. Drivers generally released the accelerator more quickly, reached full braking sooner, and applied harder braking as urgency increased. The study also reported that PRT increased, sometimes substantially, at larger headways.

The same study further reported that drivers in low-urgency scenarios more frequently performed multi-stage braking, resulting in longer delays between the initial brake application and the maximum brake pedal force reached during the braking event. The transition time from initiation to full braking varied significantly, ranging from 0.92 s to 4.21 s. In contrast, high-urgency situations resulted in more immediate and forceful braking responses.

The timing of brake initiation is also important in crash-imminent situations. Brake onset can be determined from longitudinal acceleration signals by identifying the point at which the vehicle begins to decelerate (Liu et al., 2025). A complementary measure to brake onset that is common in research is Time-To-Collision (TTC) (Vogel, 2003). TTC is defined as "the time required for two vehicles to collide if they continue at their present speeds and on the same path" (Hayward, 1972). By determining the minimum TTC during a maneuver, TTC can be used as a safety indicator of certain maneuvers (Vogel, 2003).

Compared to steering-related metrics such as SWA and SWAV, braking has been more extensively studied using real-world driving data. However, this thesis aims to broaden the perspective by identifying driver braking control limitations under different driving conditions, with a primary focus on driver input rather than the vehicle's response.

1.1.3 Crash types and vehicle actions

The type of crash scenario and preceding vehicle actions influence the driver's avoidance strategy and control inputs (Mazzae et al., 1999; Sarkar et al., 2021). In particular, different crash types are associated with distinct patterns in steering and braking behavior, which may influence the observed levels of SWA, SWAV, and deceleration.

A rear-end crash refers to a collision where a following vehicle impacts the rear of a

preceding vehicle (Dimitriou et al., 2018). Rear-end crashes have been reported to be among the most common crash types, accounting for approximately 25.0% of all crashes (Brittany N. Campbell and Najm, 2003). Driver responses in rear-end conflicts with a lead vehicle varied across crash events. In the crash subset, nearly half of the drivers showed no discernible avoidance response, while 40.0% responded by braking alone and 6.7% by combining braking and steering (S. E. Lee et al., 2007). No cases of steering alone were reported. Delayed braking is a key contributing factor in rear-end collisions, fundamentally linked to driver distraction and failures to maintain forward gaze (Zhao and Lin, 2026a). These findings suggest that driver responses in such scenarios are predominantly braking-based, with limited involvement of steering maneuvers, which may constrain steering-related measures such as SWA and SWAV.

Another frequently analyzed crash type is lane-change crashes. An analysis of the 1999 GES data found that lane-change crashes accounted for approximately 9.0% of all crashes (Sen et al., 2003). In contrast to rear-end scenarios, where avoidance responses are primarily associated with braking, lane-change situations involve lateral maneuvers that are executed through steering control (Agnvall, 2008). Consequently, steering-related measures such as steering wheel angle (SWA) and steering wheel angle velocity (SWAV) are particularly relevant for analyzing driver behavior in lane-change scenarios.

Another study, based on the 100-Car Naturalistic Driving Study, analyzed run-off-road (ROR) events and found that ROR events occur across different roadway geometries, most frequently on straight roads (56.0%), followed by curves (30.0%) and intersections (14.0%) (McLaughlin et al., 2009a). These scenarios are associated with variations in steering behavior, with intersection maneuvers generally involving larger steering inputs compared to straight roads and curves. Furthermore, approximately 50.0% of the drivers applied braking during ROR events, indicating that both steering and braking are involved in the avoidance response. This finding suggests that ROR scenarios may require a combination of lateral and longitudinal control, making both steering-related measures (e.g., SWA, SWAV) and deceleration relevant when analyzing driver performance.

Two additional studies further investigated ROR events, one using data from the General Estimates System (GES) and the Fatality Analysis Reporting System (FARS) (J.-S. Wang and Knipling, 1994), and the other using data from the 100-Car Naturalistic Driving Study (McLaughlin et al., 2009b). Both studies analyzed events occurring in right-hand traffic environments and reported a higher frequency of ROR events to the right than to the left. Specifically, the GES/FARS study reported that 40.2% of the single vehicle roadway departures occurred to the right, compared with 27.3% to the left. Similarly, the 100-Car study found that 66.0% of the ROR events occurred to the right, while 31.0% occurred to the left.

Another common traffic conflict occurs at intersections, where a subject vehicle performs a turning maneuver across opposing traffic. The Left-Turn-Across-Path

(LTAP) scenario is a significant type of intersection crash, comprising approximately 7.0% of all police-reported traffic accidents in the United States in 1991 (Chovan et al., 1994). The study reported that 80.0% of the crashes occurred on dry road surfaces and 73.0% during daylight conditions. However, these values should be interpreted as descriptive statistics, since the study did not account for the proportion of driving conducted under the corresponding conditions. The detailed crash analysis identified faulty perception and obstruction of view as the most frequently occurring causal factors, together accounting for nearly 78.0% of the LTAP crashes. In a separate test-track study investigating driver crash-avoidance behavior in an unexpected intersection-incursion scenario, 94.0% of the participants on dry pavement, and 98.0% on wet pavement applied both braking and steering to avoid a collision (Mazzae et al., 1999).

1.1.4 Road conditions

While previous sections have focused on driver inputs and resulting vehicle responses, these responses are ultimately constrained by the available tire-road friction (Yan et al., 2025). Conditions such as heavy rain, snow, and ice reduce friction, which significantly extends braking distance and may cause the vehicle to deviate from the driver's intended path. Under such conditions, even optimal driver inputs may fail to produce the expected vehicle response, as the physical limits of the road interface are reached (Fang et al., 2025).

One example of how these conditions affect driving inputs is a study on steering behavior conducted on both wet and dry pavements for unexpected obstacles (Mazzae et al., 1999). The study reported an average avoidance angle of 53.0° on dry roads and 74.0° on wet roads, while the average maximum steering rate was 262°/s and 294°/s for dry and wet pavement, respectively. Mazzae et al. (1999) also found that the highest observed SWA was 271° for dry pavement, while 289° was reported as the highest observed SWA for wet pavement. Additionally, the highest observed SWAV for dry pavements was reported as 1159 °/s and 1335°/s for wet pavements.

Another study evaluated braking performance in terms of vehicle deceleration using two cars equipped with ABS on both dry and wet asphalt surfaces (Ahrens et al., 2026). The same test course was used for both road conditions, where the vehicles first completed five laps (20 braking tests) on dry asphalt, followed by four laps after approximately 10,000 liters of water had been distributed onto the test course using a water truck. For both vehicles, the target speed was 65 km/h, and drivers were instructed to apply the brakes as rapidly and forcefully as possible upon entering the test zone. The results showed that deceleration levels on wet asphalt were significantly lower than on dry asphalt. Specifically, the average deceleration on dry asphalt was 0.902g and 0.962g for the two vehicles, respectively, while the corresponding values on wet asphalt were 0.787g and 0.818g.

The observed differences can be explained by variations in tire-road friction, which

depend on surface conditions. As shown in Table 1.1, the friction coefficients at a driving speed of 40.0 km/h vary across different road conditions, with icy roads exhibiting the lowest friction levels and wet surfaces providing less friction than dry surfaces (Novikov et al., 2018). Lower friction levels on wet or icy roads reduce the achievable vehicle response, which may lead drivers to apply larger control inputs to achieve similar maneuvers (Gillespie, 2021). This variation in friction is primarily due to changes in the contact conditions between the tire and the road surface, where water, snow, or ice reduce the effective grip available for force generation (Pacejka, 2006).

Table 1.1: Friction coefficients for different road conditions at the driving speed 40.0 km/h.

Friction coefficients		
Road condition	Dry	Wet
Asphalt or concrete	0.70–0.80	0.40–0.50
Gravel surface	0.60–0.70	0.30–0.40
Unsurfaced road	0.50–0.60	0.20–0.40
Packed snow road	0.20–0.30	0.20–0.30
Icy road	0.10–0.20	0.10–0.20

1.1.5 Lighting conditions

Traffic collisions are more frequent under reduced lighting, particularly during dusk and nighttime, compared to daylight conditions (Uttley and Fotios, 2017). Reduced illumination impairs visual performance, resulting in increased reaction times and impeded hazard detection. Previous studies have also reported an increased risk of injury-related crashes in darkness, with estimates suggesting approximately a 43.0% higher risk compared to daylight driving (Johansson et al., 2009).

Reduced lighting has also been associated with impaired lane keeping, as drivers may require more frequent steering corrections, leading to less stable driving behavior (D.Bullough et al., 2008). Furthermore, nighttime driving has been shown to delay drivers' responses to lead vehicles, resulting in less time to react. This relationship may lead to more abrupt or aggressive braking, as drivers respond later to a stopping vehicle ahead (Oliver et al., 2023).

1.2 Aim and objectives

The aim of this thesis is to quantify driver control limitations in crash-imminent situations by estimating maximum steering and braking abilities of drivers. These abilities are defined as the extent to which drivers are able to utilize steering and braking inputs under critical conditions.

This aim is further achieved by combining insights from existing literature with analysis of real-world crash data. The thesis further examines how these limitations vary across different driving conditions and how they are influenced by the presence of ADAS.

Based on these findings, the results can support and justify adaptations in the design of active safety systems to improve future crash mitigation and avoidance.

1.2.1 Research questions

To achieve this aim, the following research questions (RQs) are addressed:

- RQ1: What are the maximum steering and braking levels exhibited by drivers during crash-imminent events, and how do these values compare with previously reported findings in the literature?
  - Which performance metrics can be used to quantify driver steering and braking behavior in crash-imminent situations?
  - Which threshold values can be used to distinguish evasive steering and braking input from steering and braking events?
- RQ2: Do driver steering and braking limitations vary under different driving conditions?
  - How are driver control limitations influenced by vehicle speed, crash type, road type (e.g, intersections versus straight roads) and environmental conditions (e.g, weather and road surface)?
- RQ3: Do driver control limitations differ when ADAS are active compared to when they are inactive?
- RQ4: How can knowledge of driver control limitations be used to improve the timing of existing ADAS?

1.2.2 Objectives

In order to address the research questions, the following objectives must be met.

- Identify a subset of the database that excludes invalid data points, which are assessed to violate physical laws or fall outside thresholds reported in the literature.
- Define suitable variables to assess driver control limitations.
- Categorize the data based on existing annotations and by extracting information related to the activation of ADAS.
- Perform comparative analyses across different driving conditions, as well as between scenarios with and without ADAS.
- Apply appropriate statistical analysis methods to the data groups in order to assess statistical significance.
- To use the identified driver control limitations in a simulation environment to assess whether drivers could potentially avoid collisions at current AEB activation thresholds.
- Summarize the findings and formulate recommendations for adjustments to ADAS based on identified driver control limitations.

1.3 Scope

To maintain a clear focus and account for the nature of the available data, the following constraints apply to this thesis:

- **Driver state**
  As the database exclusively contains vehicle-specific diagnostic data, human factors such as fatigue, distraction, and stress cannot be directly evaluated.

- **Driver demographics**
  No personal information or demographic data regarding the drivers is available. Consequently, the study cannot develop personalized thresholds or perform analyzes based on demographic variables.

- **Environmental and human variability**
  The dataset does not explicitly categorize environmental conditions (e.g., specific road friction) or physiological constraints of the driver. To account for this variability, driver control limitations will be presented as intervals rather than fixed values, representing a broad spectrum of real-world driving scenarios.

2
Methodology

This chapter describes the methodology used to address the research questions and achieve the objectives of this thesis. The methodology consists of four main components: a literature review, data preprocessing, definition of maximum values and thresholds, and statistical analysis. Together, these components provide the foundation for quantifying driver control limitations.

2.1 Literature review

A literature review was conducted to provide an overview of existing research on driver control limitations and to identify benchmark values reported in the literature. These values were used as a reference for comparison with the real-world crash data analyzed in this thesis.

Scientific publications were retrieved primarily from databases such as *Scopus* and *ScienceDirect*. The literature search included both structured keyword-based searches and snowballing through the reference lists of relevant publications.

2.2 Data preprocessing

This section describes the database used to analyze real-world crash data, as well as the methods used to process and evaluate the data. It further introduces the approaches used to quantify driver control limitations.

All data processing and analysis were performed using Python (version 3.10), which enabled access to data analysis tools provided by Volvo Cars. The main libraries used included NumPy, Pandas, SciPy, Matplotlib, Seaborn, and Statsmodels.

2.2.1 Use of AI tools

AI-based tools, primarily Microsoft Copilot, were used as auxiliary support during the thesis work. Copilot was mainly used to support the identification of relevant Python functions and as coding support during parts of the script development.

In addition, several large language model tools were used to support spelling and grammar checks, language refinement, and improvements to the clarity and read-

ability of selected parts of the report. In these cases, the authors first developed the underlying analysis, text, code, and methodological reasoning independently. The AI tools were then used to request suggestions for refinement, alternative formulations, code improvements, and readability enhancements.

The use of AI tools was therefore limited to supportive and iterative tasks and did not replace the authors' own analysis, interpretation, or decision-making. All AI-generated suggestions were critically reviewed, adapted, and modified before being included in the thesis.

2.2.2 Database

The data analyzed in this thesis originate from a large database provided by Volvo Cars, containing diagnostic information from approximately two million connected vehicles. This database provides real-world crash data, enabling the analysis of driver behavior in naturalistic driving conditions.

The database contains time-series signals recorded within an eight-second window centered around an automated trigger event. These trigger events can be of different types and priorities, where crashes represent the highest priority. Other triggers include AEB activation, belt retraction, and eLKA activation. The dataset includes a range of crash types, such as rear-end collisions and lane departures, as well as events under varying driving conditions.

The signal data were enriched with contextual information through manual and semi-automated annotations derived from front dash camera footage recorded during the crash. These annotations included variables such as weather conditions and conflict type. The crash index, indicating the time point of the collision, was determined using an automated script. In cases where the result was unclear, the calculated crash index was reviewed and manually adjusted.

As the database is continuously updated, not all confirmed crash cases are fully annotated. At the time of analysis, 10,238 confirmed crash cases with available annotations were accessible and used as the basis for this thesis.

2.2.3 Data screening

The data screening focused on identifying and retrieving the signals relevant for analyzing driver control before the crash. The selected signals are summarized in Table 2.1, including their corresponding units and descriptions. Signals originally measured in radians and meters per second were converted to degrees and kilometers per hour, respectively, to improve interpretability.

The extracted data were segmented into pre-crash, post-crash, and complete crash sequences. When crash index annotations were available, the segmentation was based on the crash index. For cases without a reliable crash index, the automated

trigger point, corresponding to the midpoint of the recorded event, was used as an approximate separation point. This provided a consistent distinction between pre- and post-crash phases across the dataset.

Since impact effects may introduce unrealistic signal spikes after the collision, post-crash data were excluded when determining maximum values of driver control (Liu et al., 2025). Consequently, the analysis of driver control limitations was based only on pre-crash data, ensuring that the extracted metrics primarily reflected driver behavior rather than crash-induced artifacts.

2.2.4 Data filtering

Data filtering was applied to obtain a valid subset of crash scenarios and to reduce the influence of sensor errors, signal artifacts, and cases without usable pre-crash information. Cases were excluded if they contained inconsistent time series or if the vehicle remained stationary throughout the recorded sequence. Cases were also excluded if the crash index corresponded to the first signal sample. These cases were considered unreliable for the analysis, as they could result in incorrect time-dependent calculations, indicate missing or invalid vehicle motion, or provide no pre-crash data for extracting driver behavior.

After these initial exclusions, maximum values of SWA and SWAV were extracted from the corresponding signals. The distributions of the original signed maximum values were then examined to identify potential outliers. As shown in Figure 2.1, both distributions contained a distinct cluster at the far left, outside the expected range.

A closer examination of the cases belonging to the cluster showed that these anomalies were caused by sensor or measurement transducer failures occurring at the time of crash impact, resulting in erroneous signal values. An example is shown in Figure 2.2, where both SWA and SWAV exhibit abrupt drops at the moment of impact.

To remove cases belonging to the identified cluster, all cases with an absolute maximum SWA exceeding 680° were excluded, as such angles were considered physically unattainable and indicative of sensor errors. These cases were removed from all subsequent analysis, not only steering-related analyses, since sensor faults compromise the integrity of multiple signals.

With the outlier cluster removed, it can further be observed from Figure 2.1 that the distributions of both SWA and SWAV are largely symmetric around zero. Consequently, to ensure that both left- and right-hand steering maneuvers were treated consistently in the subsequent analysis, the absolute values of SWA and SWAV were used when identifying maximum values.

In addition to clearly invalid signal values, the distribution plots also showed cases exceeding threshold values reported in the literature. These cases were not excluded

Table 2.1: Extracted signals from the dataset.

List of signals		
Signal	Unit	Description
Acc State	-	Indicates the status of the ACC; >1 (Active), 0 (Off)
AEB activation status	-	Indicates activation of AEB; >1 (Active), 0 (Off)
Conflict situation	-	Annotated crash type (rear-end, animal, run-off-road, etc).
Crash index	-	Annotated sample corresponding to the time of the crash.
Driver deceleration request	m/s^2	Driver-related deceleration request, which includes brake system gain and therefore does not represent pure brake pedal input.
FCW request	-	Request to activate FCW; >1 (On), 0 (Off)
Global time	s	Global time, sampled at intervals of 0.1 s.
Light condition	-	Annotated lighting condition (e.g., daylight or darkness).
Longitudinal acceleration	m/s^2	Filtered longitudinal acceleration based on wheel speeds.
Longitudinal velocity	m/s	Vehicle speed relative to the ground. Negative values indicate that the vehicle is reversing.
Road condition	-	Annotated road surface condition (e.g., dry, wet).
Steer status	-	Status for autonomous driving including steering; >1 (Active), 0 (Off)
Steering wheel angle	rad	Steering wheel angle relative to the center position of the steering wheel. The signal value is signed around zero (center steering wheel position), where left turns (counterclockwise) are represented by positive values and right turns (clockwise) by negative values.
Steering wheel angle velocity	rad/s	Steering wheel angular velocity. Turning the steering wheel left (counterclockwise) is represented by positive values, and turning the steering wheel right (clockwise) is represented by negative values.
Vehicle action	-	Annotated vehicle maneuver (e.g., driving straight, turning).
Weather	-	Annotated information about the weather during the event.

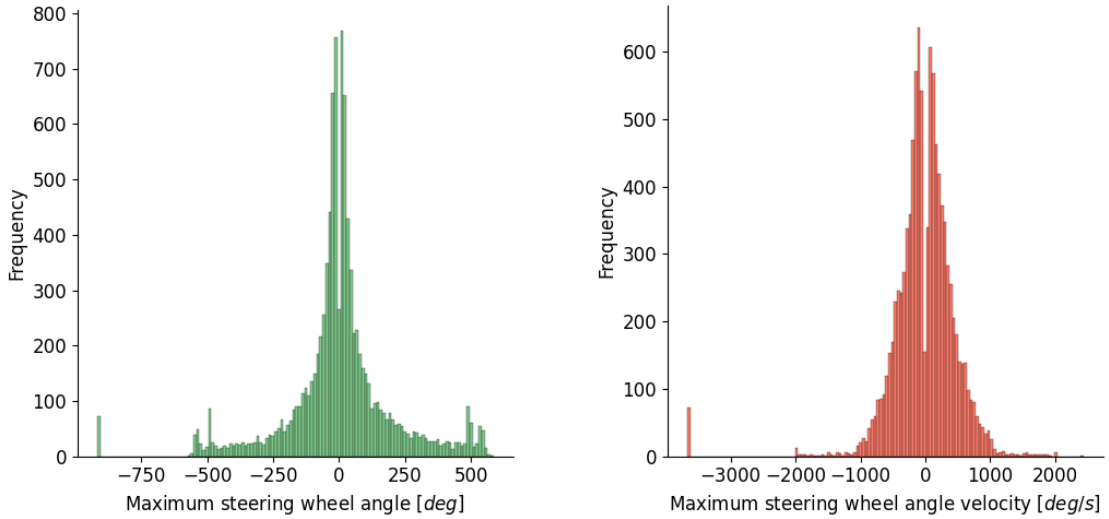

(a) Distribution of the maximum SWA with a distinct outlier cluster to the left.

(b) Distribution of the maximum SWAV with a distinct outlier cluster to the left.

Figure 2.1: Distributions of maximum SWA and SWAV before removal of outliers.

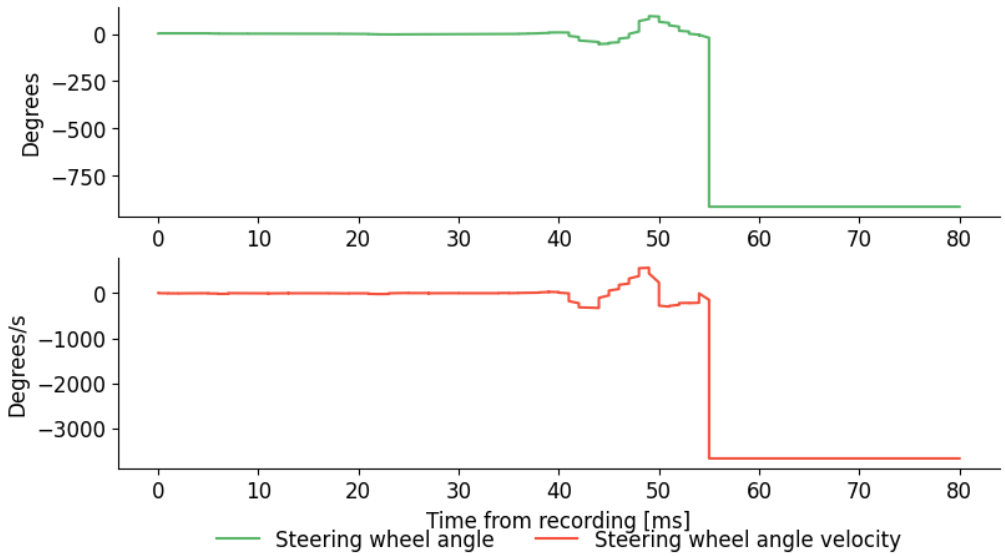

Figure 2.2: Example of a crash case demonstrating sensor failure during impact for both SWA and SWAV.

solely based on the thresholds, as high values may still represent valid driver behavior. Instead, they were reviewed to determine whether the values reflected valid pre-crash driver input or were caused by incorrect crash index assignment and post-crash effects.

A summary of the number of excluded cases and the disqualifying conditions is presented in Table 2.2. After applying all filtering criteria, the final dataset consisted of 9,829 valid cases out of the original 10,238.

Table 2.2: Total number of cases filtered out from the dataset per disqualifying conditions.

Filtering of cases	
Disqualifying condition	Number of events
Inconsistent time series	285
Damaged sensors at crash impact	72
Crash index at first samples	42
Standing still the entire sequence	4
Cases without recordings	3
Cases without images	3
Total excluded cases	409 out of 10,238
Remaining valid cases	9,829

2.2.5 Re-annotation of crash index

After the initial cleaning, some remaining cases showed implausible maximum values, exceeding values reported in the literature. These cases were reviewed to determine whether the crash index required correction. Since the crash index directly determines the separation between pre- and post-crash behavior, inaccurate annotations could substantially bias the estimation of driver control limits. This potential source of error motivated the re-annotation procedure described below.

To design the re-annotation process, an initial subset of 80 cases was independently reviewed by the two authors. This step was conducted to assess inter-rater reliability and determine whether subsequent cases could be annotated independently or required joint review. Prior to this evaluation, a set of rules was defined to ensure consistency in determining the crash index across different scenarios.

Within these rules, the *ego vehicle* refers to the vehicle under analysis, the *lead vehicle* refers to the vehicle traveling ahead of the ego vehicle, and the *following vehicle* refers to the vehicle traveling behind the ego vehicle. The general and crash-type-specific rules used for determining the crash index are described below.

For most crash types involving a collision with another road user, vehicle, animal, or object, the crash index was defined as the first sample at which the ego vehicle made

contact with the collision partner or object. This definition applied to animal, head-on, intersection, lane-change, opponent left turn ego same direction (SD), parking, rear-end (strike), straight crossing path (SCP), and vulnerable road user (VRU) crashes. The crash types requiring additional rules were rear-end (struck) and run-off-road crashes.

- *Rear-end (struck)*: Collisions in which the ego vehicle is struck from behind by a following vehicle. Since the contact point may be difficult to identify directly, the crash index was set to the first sample at which a change in direction was visible from the front dash video. If the video footage was unclear, the first change indicated in the signal data by SWA or SWAV was used. If neither was available, the first sample at which the object approaching from behind became visible was selected.
- *Run-off-road*: Events in which the ego vehicle departs from the roadway. The crash index was set to the first sample at which two wheels were assessed to be outside the roadway. If road markings were available, these were used to define the roadway boundary. Under snowy conditions, the first sample at which snow was observed being thrown up against the vehicle was selected. If the vehicle made contact with a curb or road barrier, the first sample at which the curb or barrier was touched by the front wheels was used. If it was difficult to determine the correct sample between two images, the image corresponding to a peak in SWAV was selected.

An agreement of 65.0% was achieved across the 80 mutually annotated cases when allowing a tolerance of five samples (0.125 s). When the tolerance was increased to ten samples (0.25 s), the agreement increased to 80.0%.

Most disagreements at the five-sample tolerance were associated with run-off-road events or cases with missing crash type annotations. When these cases were excluded, the inter-rater agreement increased from 65.0% to approximately 90.0%.

Based on this result, run-off-road events and cases with missing crash type annotations were considered more uncertain and were therefore annotated jointly in the subsequent re-annotation process. Cases belonging to other crash types were annotated independently, while cases for which agreement could not be reached were excluded from the final dataset.

A total of 93 cases lacked crash index annotations and were therefore manually annotated. In addition, several cases were flagged for manual review based on physically implausible or literature-based threshold-exceeding control values. This included 94 cases where the maximum SWA exceeded known vehicle limitations, 15 cases where the maximum SWAV exceeded 1200°/s, and 28 cases where the maximum deceleration exceeded 1.15g. The SWAV threshold was based on reported limits for accident avoidance maneuvers, where Blundell and Harty (2015) identified 1200°/s as a representative upper bound and Breuer (2017) and Mazzae et al. (1999) reported maximum values up to approximately 1340°/s under test conditions. The deceleration threshold was based on reported upper bounds for achievable pre-crash deceleration (Mazzae et al., 2003; Papazikou et al., 2021).

These threshold exceedances were used as indicators for manual review rather than as automatic exclusion criteria. The purpose of the review was to determine whether the extreme values reflected valid pre-crash driver behavior or whether they were caused by an incorrectly placed crash index, which could allow post-crash dynamics to be included in the pre-crash signal sequence. In cases where the extreme values originated from vehicle dynamics during or after impact, the crash index was re-annotated. Cases were only excluded if a reliable crash index could not be determined or if the signal data were considered invalid after review.

Finally, three additional cases were re-annotated following later identification as outliers, including one vehicle spin and two collisions with almost stationary vehicles. In total, 234 out of 9,829 cases (approximately 2.4%) were re-annotated based on missing crash index annotations or implausible control values exceeding literature-based thresholds. Of the re-annotated cases, 65.4% were either classified as run-off-road events or involved missing crash index annotations.

A clean subset of the database was obtained, containing relevant crash scenarios that represented valid driver behavior. Based on this subset, maximum steering and braking values could be identified to estimate driver control limitations.

2.3 Maximum values and thresholds

This section presents the methods used to evaluate maximum steering and braking inputs as indicators of driver control limitations. Threshold values are then defined to distinguish small signal fluctuations from intentional steering and braking inputs, and to separate evasive maneuvers from general steering and braking events.

2.3.1 Maximum values for steering

As introduced earlier, several variables can be used to characterize steering behavior. Following the data screening and filtering procedures, different approaches were evaluated to determine suitable metrics for quantifying steering-related driver control limitations.

The evaluated approaches included maximum SWA, relative maximum SWA, maximum SWAV, stable maximum SWAV, and maximum SWAV after applying a moving average. For each approach, the resulting distributions were examined to assess how the choice of method affected the estimated steering limits. Based on this comparison, one representative metric was selected for SWA and one for SWAV.

2.3.1.1 Relative maximum SWA

In this method, the first recorded SWA sample of each event was subtracted from the entire steering signal to express steering relative to the initial steering wheel

angle position. This approach reduced the influence of baseline steering, such as driving in a curve, and focuses on the driver's response during critical maneuvers.

2.3.1.2 Stable maximum SWAV

The stable maximum SWAV was evaluated to reduce the influence of short-lived spikes in the SWAV signal. Instead of defining the maximum based on a single sample, this method considered both the magnitude and duration of steering velocity peaks.

The absolute SWAV signal was first used to identify peaks using the SciPy function `find_peaks()`. To distinguish significant peaks from smaller fluctuations, the 90th percentile of the absolute SWAV signal was used as a threshold. For each identified peak, the area above this threshold was calculated using the SciPy function `integrate.simpson()`. Peaks with both high magnitude and sustained duration therefore resulted in larger areas, while short-lived spikes and low-amplitude fluctuations had less influence on the final measure.

The peak with the largest area was defined as the stable maximum SWAV. If no peaks were detected, the maximum SWAV was used instead. This method was introduced to avoid overestimating steering performance based on isolated single-sample peaks. The method is illustrated in Figure 2.3.

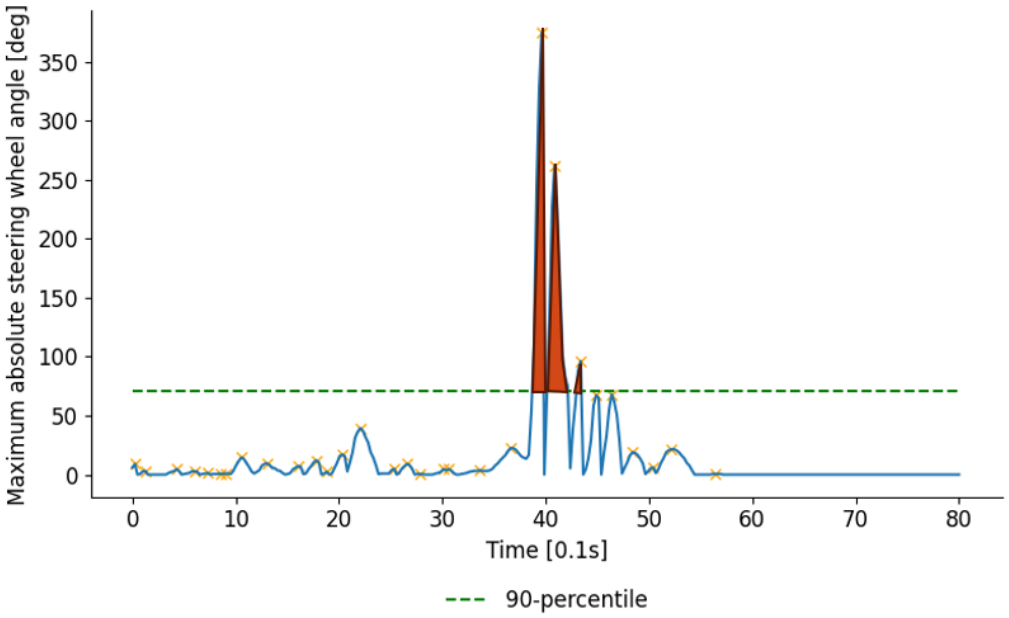

Figure 2.3: Conceptual illustration of the area-based method used to identify the stable maximum SWAV.

2.3.1.3 Maximum after moving average

The maximum SWAV after moving average was evaluated to reduce the influence of short-lived noise in the SWAV signal while preserving the overall signal shape. In this method, a moving average filter was applied before extracting the maximum absolute SWAV value.

The moving average was computed using a centered window of size $w = 5$ samples. This window size was selected as a trade-off between excessive filtering, which may attenuate true maximum values, and insufficient filtering, which may retain noise in the signal. For each sample n, the filtered value was calculated as the average of the surrounding samples within the window, according to the following equation:

$$\frac{(n-2)+(n-1)+n+(n+1)+(n+2)}{w}$$

At the signal boundaries, where the full window could not be applied, the window size was reduced, and the average was computed using the available samples. This principle is illustrated in Figure 2.4.

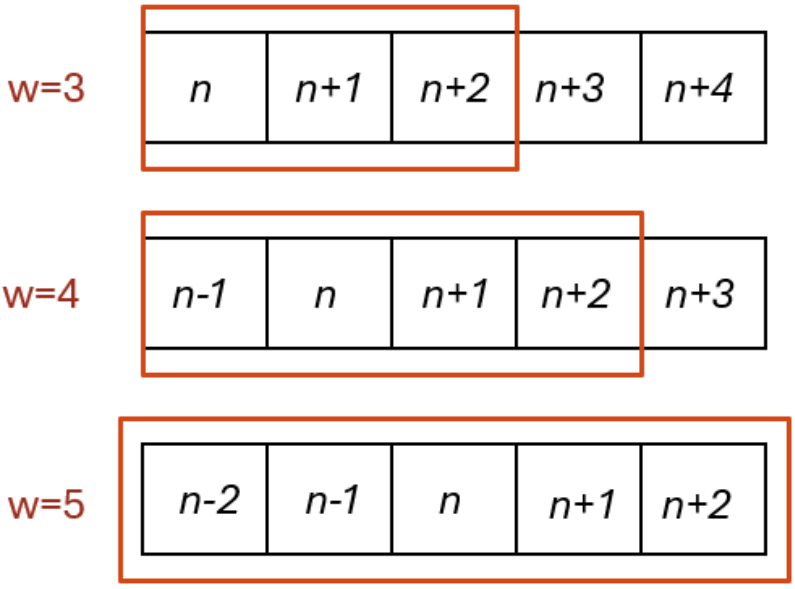

Figure 2.4: Illustration of the principle used to reduce the moving average window size at signal boundaries (edge cases).

2.3.2 Comparison of maximum steering estimation methods

The resulting distributions obtained using the different steering estimation methods were compared to assess their suitability. The comparisons were performed using kernel density estimation (KDE) applied to violin plots, with Seaborn's bandwidth adjustment set to bw_adjust = 0.3. This choice preserved the overall shape of the

distributions without excessive smoothing, while still allowing the underlying data structure to be interpreted without emphasizing individual peaks. The same bandwidth setting was used for all subsequent violin plots to ensure consistency.

As shown in Figure 2.5, the normal and relative maximum SWA methods resulted in similar distributions. This similarity indicated that both extraction approaches captured comparable steering control limits. However, the relative maximum SWA included a small number of extreme values above 600.0° (60 out of 9,829 cases).

These extreme values mainly occurred in cases where the driver applied large steering inputs in both directions within a short time interval. Among these cases, 73.0% were associated with parking maneuvers, such as entering or exiting a parking space, while 22.0% corresponded to run-off-road events. The remaining cases represented other scenarios, including potential vehicle skidding.

Given the overall similarity between the distributions and the additional extreme values introduced by the relative method, the normal maximum SWA was selected as the representative measure of steering wheel angle limitations.

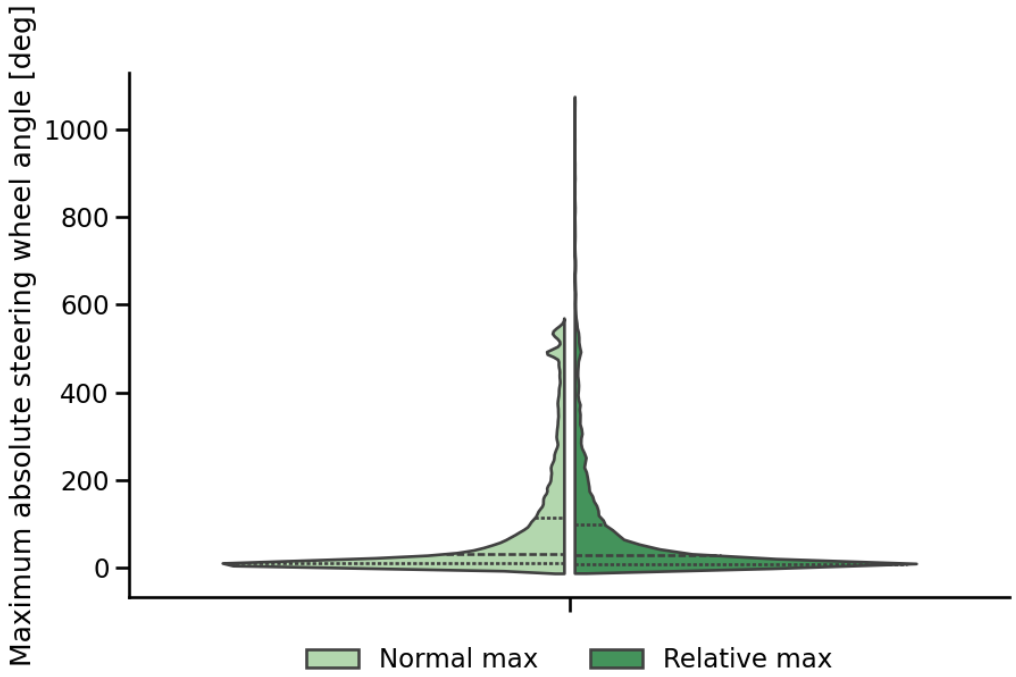

Figure 2.5: Kernel density distributions (KDE) of maximum SWAV obtained using the normal and relative extraction methods, estimated using Seaborn's bw_adjust=0.3. The distributions are similar overall, although the relative method results in slightly higher extreme values.

A similar comparison was performed for SWAV, as shown in Figure 2.6. The normal maximum SWAV and stable maximum SWAV resulted in highly similar distributions in both spread and central tendency, as shown in Figure 2.6a. This indicates that the stable interval approach did not substantially affect the estimated max-

imum values. In contrast, the moving average method resulted in systematically lower values, as shown in Figure 2.6b, suggesting that the smoothing process attenuated peak steering velocities.

Based on these results, the normal maximum SWAV was selected as the representative measure of steering wheel angle velocity.

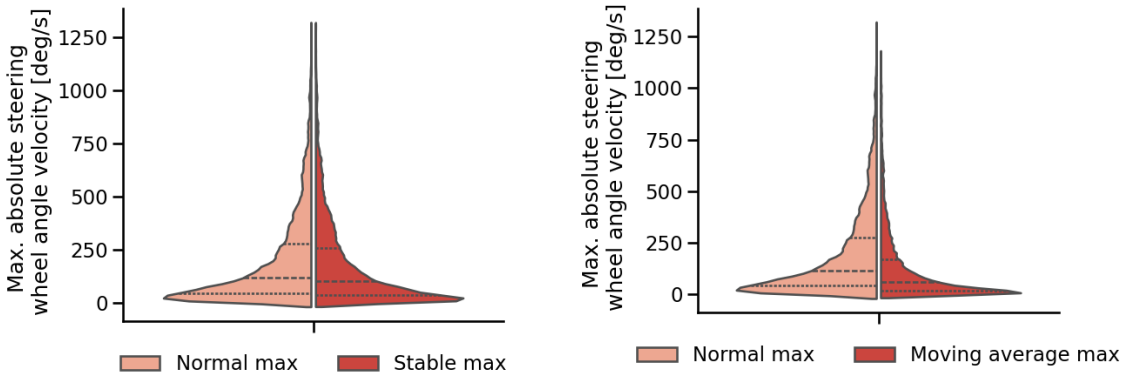

(a) Comparison of maximum SWAV and stable SWAV.

(b) Comparison of maximum SWAV and moving average maximum SWAV.

Figure 2.6: Kernel density distributions (KDE) of maximum SWAV obtained using different methods, estimated using Seaborn's bw_adjust=0.3. The figure shows similar distributions for the normal and stable maximum methods and lower values for the moving average method.

2.3.3 Maximum values for braking

Similar to steering behavior, braking can be characterized in several ways depending on the aspect of interest. In this thesis, braking behavior was analyzed using both the driver deceleration request (DDR) and the vehicle's actual longitudinal deceleration. DDR was used as an indirect measure of driver-related braking demand rather than as a direct measure of brake pedal input. This distinction is important since the available DDR signal includes brake system gain. Therefore, the signal cannot be used to separate the driver's sole pedal input from the resulting requested deceleration. For this reason, actual vehicle deceleration was also included to describe the physical vehicle response. In addition to identifying maximum braking levels, the analysis also considers the frequency and duration of braking events, as well as the timing of braking in relation to the crash.

2.3.3.1 Maximum DDR

Maximum braking demand was first evaluated using the DDR. The signal represents a bounded deceleration request in the range of 0–100%, where 100% corresponds to the maximum available request within the signal. However, DDR should not be interpreted as pure brake pedal input, since the signal includes brake system gain. Instead, it was used as an indirect indicator of driver-related braking demand in the pre-crash sequence. The maximum DDR was therefore defined as the highest recorded DDR value before the crash and could be extracted without additional signal processing.

To provide a more comprehensive description of driver braking behavior, two additional measures were considered: the number of braking events prior to the crash and the proportion of the braking sequence during which maximum braking was applied.

2.3.3.2 Maximum vehicle deceleration

The DDR alone does not fully describe the braking process, as the vehicle's actual response may differ due to system dynamics and external conditions. Therefore, the vehicle's physical deceleration was also included in the analysis.

2.3.3.3 Timing of braking

In addition to braking magnitude, the timing of the braking maneuver plays a critical role in collision avoidance. Since the available data did not allow the moment at which the driver perceived the threat to be determined, the perception–reaction time (PRT) could not be evaluated. Although time-to-collision (TTC) is commonly used to relate brake onset to crash urgency, it is a predictive measure. Given the retrospective nature of this study and the availability of crash index annotations, the actual-time-to-collision (ATTC) was instead defined to evaluate the timing of braking.

ATTC was defined as the time interval between the crash index and the onset of the last detected braking sequence exceeding 0.500 m/s^2 before the crash. This threshold was used to distinguish more pronounced braking events from minor corrective speed adjustments (Deligianni et al., 2017). An example of how ATTC was calculated is shown in Figure 2.7

2.3.4 Threshold definitions and maximum values

After selecting the representative steering and braking metrics, threshold values were defined to separate small signal fluctuations from steering and braking events, and to distinguish evasive maneuvers from more general steering and braking inputs. These thresholds were used both to generate distributions representative of driver control limitations and in the subsequent statistical analyses.

For each variable, two distributions were generated: one excluding noise and one isolating evasive maneuvers. In this context, noise refers to small fluctuations in the measured signals that may occur even during straight driving at constant velocity. Evasive maneuvers refer to steering and braking inputs that exceed the threshold values described below.

For SWA, threshold values were defined based on previous studies. To remove noise and minor steering corrections, cases with a maximum SWA below 6.0° were excluded, as such values are generally associated with measurement noise or driver

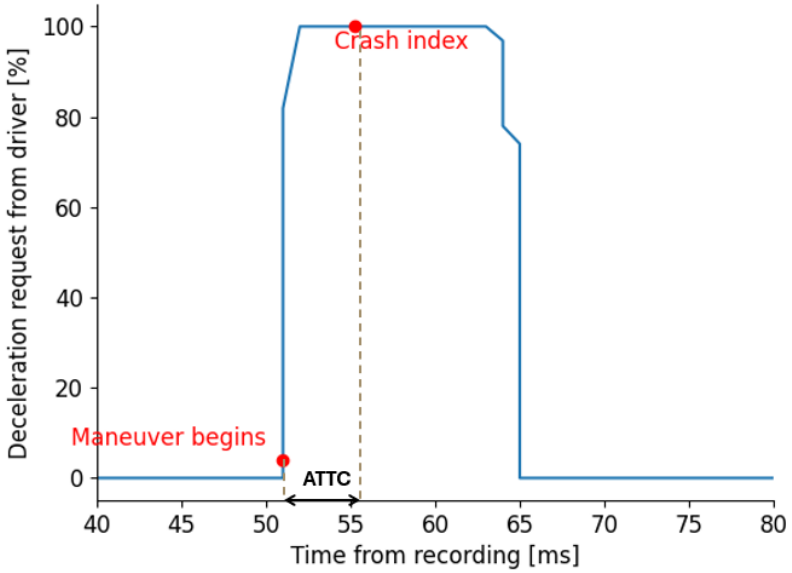

Figure 2.7: Illustration of the principle used to calculate the ATTC.

micro-adjustments (McGehee et al., 2004). As introduced earlier, Planek et al. (2014) reported maximum SWA values of approximately 40.0° for standard overtaking maneuvers. Accordingly, values above 40.0° were classified as evasive maneuvers in this study.

A limited sensitivity analysis was performed to evaluate the robustness of the selected SWA thresholds and their influence on the 95th percentile estimates. For the lower steering threshold, the selected value of 6.0° was varied by ±5.0°, resulting in tested thresholds of 1.0° and 11.0°. The corresponding 95th percentile estimates ranged from 449° to 487°, compared with 473° for the selected threshold. For the evasive steering threshold, the selected value of 40.0° was varied by ±5.0°. The corresponding estimates ranged from 497° to 500°, compared with 498° for the selected threshold.

Similarly, the SWAV threshold values were established based on the literature. To reduce the influence of noise and small fluctuations, a lower threshold of 3.0°/s was applied, below which steering activity was considered insignificant (SAE International, 2013). For evasive SWAV, Blundell and Harty (2015) reported that values in the range of 0–400°/s are representative of normal driving conditions, while Breuer (2017) identified 292°/s as the lowest maximum value observed during evasive maneuvers. Based on these findings, a threshold of 300°/s was adopted to identify evasive steering inputs. This value lies slightly above the lower bound reported for evasive maneuvers while remaining within the upper range reported for normal driving.

A limited sensitivity analysis was also performed to evaluate the robustness of the selected SWAV thresholds. Since the lower threshold of 3.0°/s is close to zero, a

practical range between 1.0°/s and 10.0°/s was evaluated instead of applying a symmetric variation. The corresponding 95th percentile estimates ranged from 636°/s to 645°/s, compared with 638°/s for the selected threshold. For the evasive SWAV threshold, the selected value of 300°/s was varied by ±10.0°/s. The corresponding estimates ranged from 855°/s to 864°/s, compared with 859°/s for the selected threshold.

For DDR, the same noise-reduction procedure described in Varotto et al. (2021) was applied. Specifically, deceleration values below 0.50 m/s^2 were excluded, as such values are generally associated with minor corrective speed adjustments rather than more pronounced braking events. Thresholds for evasive braking were subsequently defined based on established deceleration criteria reported in the literature. Intentional braking is commonly associated with deceleration values in the range of 2.50–3.50 m/s^2 (Saptoadi, 2017). In addition, the Institution of Transportation Engineers (ITE) recommends 3.0 m/s^2 as a representative threshold for normal braking, while the American Association of State Highway and Transportation Officials (AASHTO) suggests 3.40 m/s^2 as a comfortable deceleration level. Based on these references, a threshold of 3.0 m/s^2 was adopted to identify evasive braking events.

No additional sensitivity analysis was performed for DDR, as the corresponding 95th percentile values remained at the upper system limit of 100% for both general braking events and evasive braking events. This indicated a ceiling effect in the DDR signal, where a large proportion of drivers reached maximum brake request, making the resulting percentile estimates largely insensitive to moderate variations in the selected threshold definitions.

Finally, the 95th percentile was used to represent the upper limits of the selected variables. Percentile values were calculated separately for the noise-filtered distributions and for the subsets representing evasive maneuvers. Consequently, each evasive maneuver distribution constituted a subset of the corresponding noise-filtered distribution. This approach reduced the influence of extreme outliers while still capturing high levels of driver control performance across the population (Uddin et al., 2024). The use of the 95th percentile is also consistent with the design philosophy of ADAS, which are developed based on population-level characteristics rather than individual driver behavior.

2.4 Statistical analysis

This section describes the methodology used to evaluate whether different driving conditions and the activation of ADAS have a statistically significant effect on the maximum values of SWA, SWAV, DDR and ATTC.

2.4.1 The effect of different driving conditions

The driving conditions considered in this analysis include speed groups, crash types, vehicle actions, road condition, and lighting conditions. These variables were selected to capture key contextual factors that may influence driver behavior in critical situations.

2.4.1.1 Speed groups

Crash types, vehicle actions, road conditions and lighting conditions were obtained directly from the dataset annotations. Vehicle speed, however, varies over time and was therefore extracted at the time point corresponding to the maximum value of the analyzed maneuver. For example, in the analysis of SWAV, vehicle speed was paired with the time at which SWAV reached its maximum. Since ATTC is derived from the braking sequence rather than a maximum value, ATTC was analyzed in relation to the speed group corresponding to the maximum DDR.

The extracted speeds were categorized into six groups: 0–10, 10–30, 30–60, 60–80, 80–120, and 120–200 km/h. These categories were selected to reflect typical speed limits associated with different road types:

- 0-10: Walking speed is defined as 5.0-7.0 km/h (Trafikverket, 2011). This group represents driving at walking speed, including parking maneuvers and reversing.
- 10-30: Represents driving in areas with a high presence of vulnerable road users (VRUs), where vehicle speeds are regulated at 30.0 km/h (Trafikverket, 2011).
- 30-60: A speed limit of 50.0 km/h is standard for urban roads in Sweden, although a reduction to 40 km/h has been proposed by the authority Trafikanalys (Trafikverket, 2025; Union, 2024). Speed limits are assigned on a per-road basis and may vary in increments of 10.0 km/h (Trafikverket, 2025).
- 60-80: A speed limit of 70.0 km/h is standard for rural roads in Sweden; however, limits of 60 km/h and 80 km/h are also commonly applied (Trafikverket, 2025; Union, 2024).
- 80-120: A speed limit of 110 km/h is standard for motorways in Sweden, while 120 km/h is the highest permitted limit (Trafikverket, 2025; Union, 2024).
- 120-200: This speed group exceeds the national speed limits but was included to account for speeding behavior. In Sweden, 80.5% of drivers report exceeding motorway speed limits at least once during a 30-day period, which is the highest reported rate among European countries included in the survey (Holocher and Holte, 2019).

2.4.1.2 Vehicle actions

Vehicle action was obtained from the dataset annotations and included categories such as driving straight, reversing, drifting out of lane or roadway, turning left or right, leaving the lane or road, and driving in lane. Categories labeled as *"something else"* or *"undefined"* were excluded due to limited interpretability, while the

remaining categories were retained for further analysis.

The vehicle action categories "Left its lane or road to the left", "Left its lane or road to the right", and "Drifting out of lane" were merged into a single category "Lane departure", as these labels represent the same vehicle action but were used in different versions of the dataset.

To assess whether other vehicle action categories could be merged, post-hoc pairwise tests were performed. For SWA and SWAV, which were found to be normally distributed, Independent-samples t-tests were conducted using SciPy `ttest_ind()`. For DDR and ATTC, which did not exhibit normality, Mann-Whitney U-tests were conducted using SciPy `mannwhitneyu()`. Because multiple pairwise comparisons were performed, a Bonferroni correction was applied to reduce the risk of false-positive results (Armstrong, 2014). The corrected significance level was obtained by dividing $\alpha = 0.05$ by the number of pairwise comparisons within each analysis.

Vehicle action categories were subsequently merged only if they exhibited no statistically significant differences across all four variables and were judged to represent similar driving patterns. Categories with statistically significant differences were retained as separate groups.

The resulting merged vehicle action categories were then used to evaluate whether vehicle action was associated with driver control limitations. In this analysis, only values exceeding the previously defined thresholds for evasive driving were included, in order to focus on driver control limits rather than general driving behavior.

For statistically significant results, Cohen's d was calculated to assess the magnitude of the differences between groups. This was considered important due to the large sample size, where statistical significance may occur even when the practical effect is small. Cohen's d therefore provided a complementary measure of effect size and was calculated using Equations (2.1) and (2.2). According to established conventions, d-values of 0.20, 0.50, 0.80 and 1.30 correspond to small, medium, large and very large effect sizes, respectively (D. K. Lee, 2016; Sullivan & Feinn, 2013).

$$\textit{Cohen's } d = \frac{\bar{X}_1 - \bar{X}_2}{s_{pooled}} \tag{2.1}$$

$$s_{pooled} = \sqrt{\frac{(n_1 - 1)s_1^2 + (n_2 - 1)^2 s_2^2}{n_1 + n_2 - 2}} \tag{2.2}$$

($\bar{X}_i, s_i^2, n_i$: Mean, variance and sample size of group i)

2.4.1.3 Crash types

The original dataset included several annotated crash type categories, describing the general conflict scenario and collision configuration. The crash types used in the analysis were defined as follows:

- *Animal*: Collisions involving an animal.
- *Head on*: Collisions in which the ego vehicle and another vehicle collide front-to-front.
- *Intersections*: Collisions occurring in intersections, typically involving one vehicle turning while another vehicle continues straight.
- *Lane-change*: Collisions related to a lane-change maneuver, where one vehicle moves laterally into or across another vehicle's path.
- *Opponent left turn, ego same direction (SD)*: A specific intersection-related scenario in which the ego vehicle travels straight while another vehicle traveling in the same general direction performs a left-turn maneuver, resulting in a collision.
- *Parking*: Collisions occurring in parking lots, driveways, parking garages, or during parking-related maneuvers such as entering, exiting, or parallel parking.
- *Rear-end (strike)*: Collisions in which the ego vehicle strikes a lead vehicle or another object in front of it.
- *Rear-end (struck)*: Collisions in which the ego vehicle is struck from behind by a following vehicle.
- *Run-off-road*: Events in which the ego vehicle departs from the roadway, for example by leaving the lane, crossing the road boundary, or making contact with roadside elements.
- *Straight crossing path (SCP)*: Intersection-related collisions in which the ego vehicle travels straight and is struck or crossed by another vehicle moving laterally across its path.
- *Vulnerable road user (VRU)*: Collisions involving vulnerable road users, such as pedestrians, cyclists, or e-scooter users, excluding motorcycles and mopeds.
- *Other*: Crash scenarios that did not fit into the predefined crash type categories or were insufficiently specified.

The category *"Other"* was excluded from the statistical crash type analyses and distribution comparisons, as it represents a broad and insufficiently specified grouping with limited interpretability. Since the objective was to assess differences in steering and braking behavior across clearly defined crash scenarios, only well-defined categories were considered appropriate for further analysis. However, *"Other"* was retained during exploratory analyses of extreme steering events in order to identify potential patterns among the most severe maneuvers.

To evaluate whether certain crash type categories could be merged, the same statistical analysis procedure as described for vehicle actions was applied. Based on the results of this analysis, crash type categories that exhibited statistically significant differences were treated as distinct. In contrast, categories that did not show statistically significant differences across the evaluated variables and were judged to represent similar crash dynamics were merged into combined groups.

Finally, the merged crash type categories were analyzed using the same statistical framework as applied to vehicle actions to assess whether statistically significant relationships existed between crash type and driver control limitations.

2.4.1.4 Road conditions

The original dataset included the following annotated road condition categories: *dry*, *wet*, *snow/icy*, *gravel*, *uncertain*, *something else*, and *undefined*. In contrast to the vehicle action and crash type categories, the number of road condition categories was limited. Therefore, no merging or grouping analysis was performed, and the categories were initially retained in their original form.

Categories with limited interpretability were excluded from the analysis. Specifically, *uncertain*, *something else*, and *undefined* were removed, as they do not represent clearly defined road surface conditions. Since the objective was to assess the influence of road surface conditions on steering and braking behavior, only well-defined and interpretable categories were considered appropriate.

The category *gravel* was also excluded due to its small sample size ($n = 31$), which was considered insufficient to support reliable statistical comparisons with the remaining categories: *dry* ($n = 6698$), *wet* ($n = 897$), and *snow/icy* ($n = 666$).

The final road condition categories included in the statistical analysis were therefore *dry*, *wet*, and *snow/icy*. These categories were analyzed using the same statistical framework as described for vehicle actions, in order to evaluate whether statistically significant relationships existed between road conditions and driver control limitations.

2.4.1.5 Lighting conditions

The original dataset included the following annotated lighting condition categories: *daylight*, *darkness*, *darkness – street lighting*, *dusk/dawn*, *tunnel*, *something else*, and *undefined*. Categories with limited interpretability were excluded from the analysis. Specifically, *something else* and *undefined* were removed, as they represent broad and ambiguous groupings that do not correspond to clearly defined lighting conditions. The category *tunnel* was also excluded due to its small sample size ($n = 2$), which was considered insufficient to support meaningful statistical analysis.

The two groups, "darkness" and "darkness-street lighting" were merged into a single category, "darkness", as they were considered to represent the same condition in the context of this analysis.

The final lighting condition categories included in the statistical analysis were therefore *daylight*, *darkness*, *dusk/dawn*. These categories were analyzed using the same statistical framework as applied to vehicle actions, in order to assess whether statistically significant relationships existed between lighting conditions and driver control limitations.

2.4.2 The effect of ADAS activation

To examine whether driver control limitations differed depending on ADAS activation, a binary indicator was assigned to each case. This indicator specified whether any ADAS function was activated during the event sequence. The ADAS functions considered in this study were Forward Collision Warning (FCW), Lane Keeping Assist (LKA), Automated Emergency Braking (AEB), and Adaptive Cruise Control (ACC).

For each ADAS function, cases with activation were compared with cases without activation. For example, cases with AEB activation were compared with cases without AEB activation, and the same procedure was applied for FCW, LKA, and ACC. Violin plots were used to visually assess differences in the distributions of the selected driver control metrics. This analysis was exploratory and aimed to investigate whether ADAS activation was associated with differences in maximum steering or braking behavior before the crash.

When notable differences were observed, additional descriptive analyses were performed to support the interpretation of the results. For example, the distribution of speed groups was examined for cases with and without ACC activation to assess whether observed differences in steering behavior could be related to differences in driving context.

2.5 Simulation

After the maximum driver control limitations had been identified, selected limits were implemented in the open-source simulation framework esmini. Esmini executes scenarios defined using OpenSCENARIO XML files and was used to evaluate how different steering capability assumptions may influence the possibility of avoiding a crash (esmini, 2026).

A rear-end (strike) scenario was selected for the simulation, as rear-end collisions represent the most common crash type (Brittany N. Campbell & Najm, 2003). The predefined OpenSCENARIO file *straight_500m.xosc* was used as the base scenario. This scenario represents a straight-road rear-end crash configuration in which the ego vehicle approaches a stationary lead vehicle from an initial distance of 500 m. The ego vehicle was adjusted to match the specifications of a Volvo XC90.

To increase the realism of the simulated steering behavior, the steering wheel angle trajectory was extracted from an actual rear-end (strike) crash case. The selected case involved an ego-vehicle impact speed of approximately 40 km/h and a clearly identifiable steering maneuver intended to avoid a stationary lead vehicle on a straight road. This made the case suitable for adaptation to the selected OpenSCENARIO configuration.

The ego-vehicle speed was initially set to 40 km/h, based on the study by Abatan et al. (2026), which used this speed when evaluating TTC thresholds for AEB activation across 17 automakers. In the same study, AEB activation occurred at a TTC of 0.96 s, while FCW occurred 1.76 s before impact. In addition, Zhao and Lin (2026b) reported a recommended TTC threshold of 1.4 s for ADAS activation based on guidelines from the Japan Ministry of Land, Infrastructure, Transport and Tourism. These TTC values were used as baseline activation points in the simulation.

The extracted SWA trajectory was truncated to include only the active steering maneuver, from steering onset until the maneuver was completed. This allowed steering to be initiated at the selected activation points in the simulation. The trajectory was then scaled to represent different levels of driver steering limitations. The steering wheel ratio was adjusted to reflect vehicle-specific characteristics of a Volvo XC90, with a lower ratio applied for SWA values exceeding 400 ° and a higher ratio applied below this threshold. Based on these modified trajectories, OpenSCENARIO XML files were generated and executed in esmini to simulate the different steering-limit cases.

The same TTC thresholds were subsequently used to evaluate AEB performance within the same scenario. AEB activation was simulated in the scenario file using a linear speed reduction action with two deceleration levels: -9.27 m/s^2 and -7.19 m/s^2. These values were selected based on maximum deceleration levels reported in Kidd et al. (2023).
To assess whether the results were sensitive to vehicle speed, an additional simulation was performed at 70 km/h for both the steering maneuver and the AEB scenarios.

3
Results

This chapter presents the results of the statistical analyses conducted to identify maximum values of driver control limitations. The chapter begins by presenting the category-merging process and clarifying which factors were retained for the subsequent analyses. Thereafter, the maximum driver control limitations are reported for steering wheel angle (SWA), steering wheel angle velocity (SWAV), driver deceleration request (DDR) and actual time-to-collision (ATTC), together with their dependence on driving conditions and ADAS activation.

3.1 Merging of categories

The results of the omnibus testing conducted to evaluate whether specific categories could be merged and to determine the appropriate grouping structure are presented in this section. Since the road condition and lighting condition variables consisted of a limited number of well-defined and distinct categories, these driving conditions did not require merging and were therefore excluded from the category-merging analysis presented in this section.

3.1.1 Vehicle action

For vehicle action, 28 pairwise tests were conducted with a Bonferroni-corrected significance level of $0.05/28 \approx 0.0018$. The vehicle action groups that did not exhibit statistically significant differences across all four variables and were assessed to represent similar driving patterns were "Driving straight" and "Driving in its lane". These categories were merged into a single category denoted as "Lane keeping". The final set of vehicle action categories included Lane keeping, Lane departure, Turning left, Turning right, and Reversing.

3.1.2 Crash types

For crash type, 91 pairwise tests were conducted with a Bonferroni-corrected significance level of $0.05/91 \approx 0.00055$. With this significance level, the categories "LTAPOD/RTAPOD", "LTAPLD/RTAPLD" and "U-Turn" were merged into a single category denoted as "Intersections" before continuing with the analysis. The final set of crash type categories included Intersections, Straight crossing path (SCP), Run-off-road, Lane change, Animal, Parking, Opponent left turn, ego same direction (SD), Head-on, Rear-end (strike), Rear-end (struck), and Vulnerable road users (VRU).

3.2 Steering wheel angle

In this section, the results of the SWA analyses are presented, including the estimated maximum driver control limitations for both steering events and evasive steering events, as well as the influence of different driving conditions.

While differences can be observed across speed groups, crash types, and road conditions, these factors generally exhibit small effect sizes. In contrast, vehicle actions show substantially larger effect sizes, particularly between lane keeping and turning events.

Furthermore, LKA and ACC exhibit a noticeable influence on SWA compared with AEB and FCW.

3.2.1 Maximum values and distributions

The distribution of SWA, excluding values below 6° (considered as noise or non-maneuvering), is shown in Figure 3.1 in light green. The distribution is right-skewed, with a high concentration of cases at relatively small steering angles and a decreasing frequency for larger steering inputs. The 95th percentile is 473.3°.

To isolate more pronounced steering maneuvers, a subset of the data was defined using a threshold of SWA $> 40°$ (shown in darker green). This subset represents characteristic evasive steering behavior, where lower-magnitude inputs are excluded. For this subset, the 95th percentile reaches 498.1°, which serves as the representative upper-limit estimate of steering magnitude observed in the crash data. Approximately 53.7% of the steering events exceed the threshold of SWA $> 40°$, and the highest observed maximum SWA was 557°.

The corresponding distributions of vehicle actions and crash types for SWA values above 6° are shown in Figure 3.2a. Driving straight constitutes the largest proportion of cases, while drifting and turning maneuvers represent smaller shares. In terms of crash types, rear-end (strike) collisions dominate, followed by run-off-road and rear-end (struck) events.

For higher steering angles (SWA $> 40°$), shown in Figure 3.2b, a clear shift in the distribution is observed. The proportion of driving straight decreases, while drifting and turning maneuvers increase. In addition, run-off-road events become more prevalent, whereas both rear-end (strike) and rear-end (struck) collisions decrease in relative frequency.

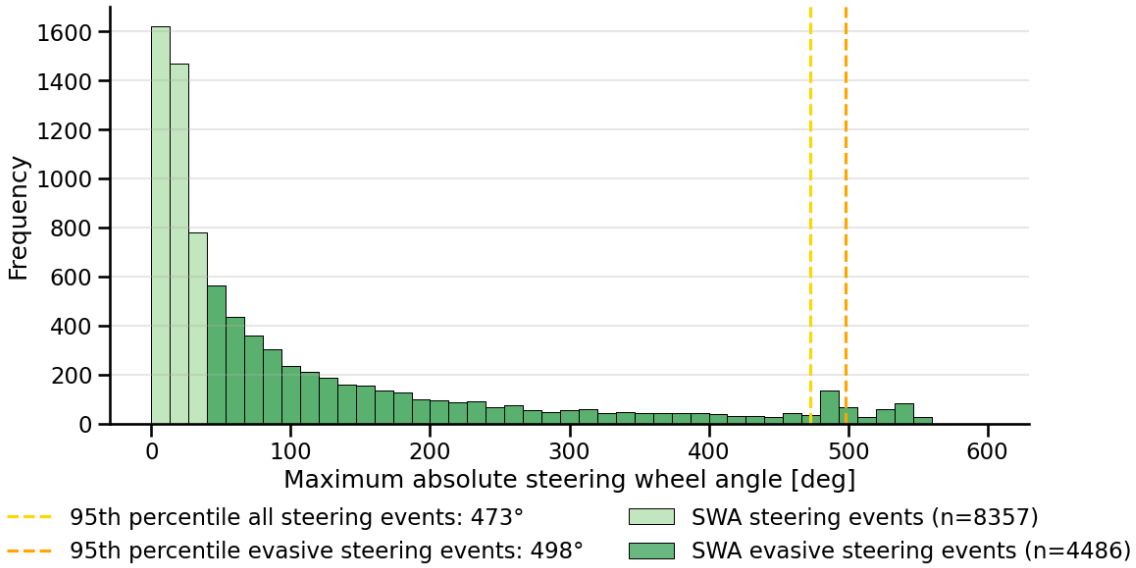

Figure 3.1: Distribution of maximum SWA for steering events above 6° and evasive steering events above 40°, including the corresponding 95th percentiles.

3.2.2 Speed groups

SWA exhibited statistically significant differences across most speed group comparisons. Exceptions were observed among the three highest speed group comparisons (60-80 vs. 80-120, 60-80 vs. 120-200 and 80-120 vs. 120-200), where no significant differences were found. These trends are visible in Figure 3.3. However, despite statistical significance, the associated effect sizes were small (mean d=0.13, range 0.01-0.21), corresponding to limited differences in steering magnitude across speed groups.

3.2.3 Vehicle actions

When examining SWA for post-hoc testing, *Reversing* was unexpectedly the only vehicle action that did not exhibit statistically significant differences when compared with any other vehicle action. Instead, the largest steering-related differences were observed between *lane keeping* and turning events, with very large effect sizes for *turning left* (d=1.4) and *turning right* (d=1.3). Additionally, a large effect size was identified between *lane departure* and *turning left* (d=1.0), indicating substantially different steering demands among these vehicle actions. However, this discrepancy in effect size was only observed for turning left and not turning right.

3.2.4 Crash types

In the post-hoc testing for crash types, statistically significant differences were observed across most crash types, however, the associated effect sizes were generally small. One crash type that nonetheless stood out was *Intersection*-related crashes,

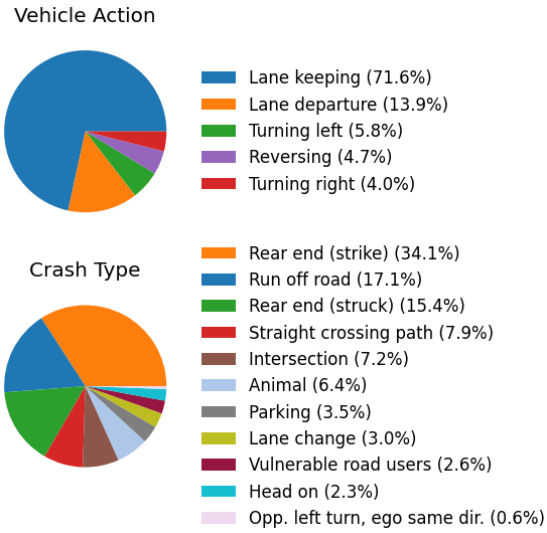

(a) Crash types and vehicle actions for SWA above 6°.

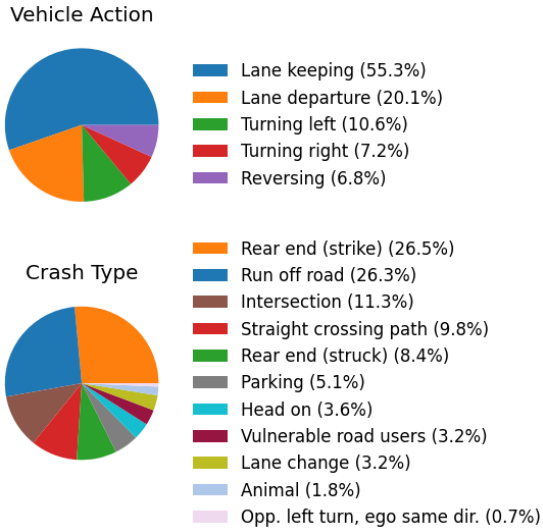

(b) Crash types and vehicle actions for SWA above 40°.

Figure 3.2: Crash type and vehicle action distributions for normal and evasive SWA.

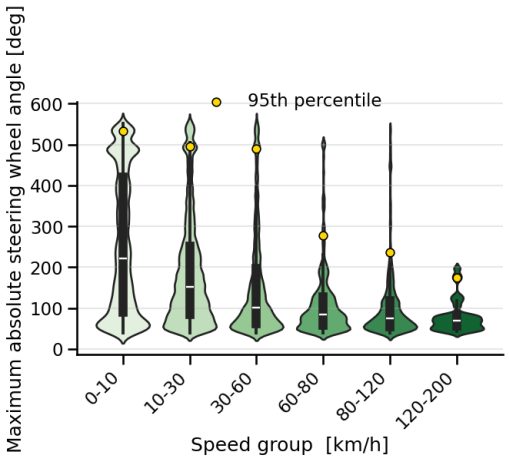

(a) Kernel density distributions (KDE) of maximum SWA across speed groups, estimated using Seaborn's violin plot with an adjusted KDE bandwidth setting (`bw_adjust = 0.3`). Yellow markers indicate the corresponding 95th percentile values, white line markers represent the mean, and black boxes represent the interquartile range with whiskers.

Speed group	Frequency	Mean value	95% percentile	Confidence interval
0-10	1252	246	532	237-256
10-30	1548	191	496	185-198
30-60	1149	155	490	148-163
60-80	289	111	277	101-120
80-120	215	104	236	92.0-115
120-200	33	81.0	175	67.0-95.0

(b) The table summarizes the sample size, mean SWA, 95th percentile, and confidence interval for each speed group.

Figure 3.3: Relationship between speed group and SWA.

which exhibited a moderate effect size (mean d=0.55, range 0.29-0.86).

3.2.5 Road conditions

For road conditions, one category consistently stands out from the others: *snowy/icy* road conditions. This road condition exhibited statistically significant differences for all evaluated variables except for driver deceleration request when compared with the two other road conditions.

For steering behavior, the effect sizes associated with road condition were small but still consistent. Snowy and icy road conditions exhibited a small effect size for both dry roads (d=0.1) and wet roads (d=0.2), indicating slightly increased steering activity under reduced-friction conditions as shown in Figure 3.4.

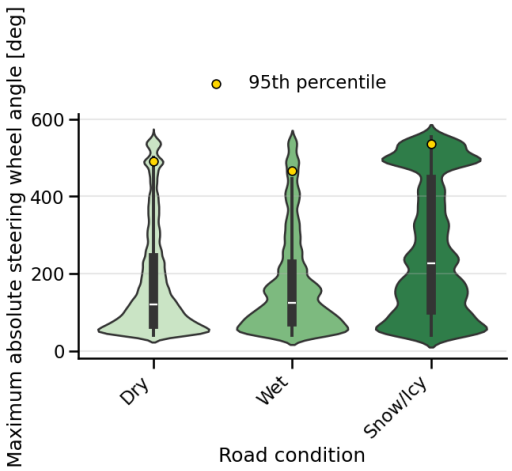

(a) Kernel density distributions (KDE) of maximum SWA across road conditions, estimated using Seaborn's violin plot with an adjusted KDE bandwidth setting (`bw_adjust = 0.3` = 0.3). Yellow markers indicate the corresponding 95th percentile values, white line markers represent the mean, and black boxes represent the interquartile range with whiskers.

Road condition	Frequency	Mean value	95% percentile	Confidence interval
Dry	2908	178	490	172-183
Wet	412	172	467	160-185
Snow/icy	453	264	535	248-280

(b) The table summarizes the sample size, mean SWA, 95th percentile, and confidence interval for each road condition.

Figure 3.4: Relationship between road condition and SWA.

3.2.6 Advanced driver assistance systems

For evasive SWA ($> 40°$), AEB and FCW showed limited influence on the distribution, while LKA is associated with lower steering magnitudes, as shown in Figure 3.5. In contrast to AEB and FCW, LKA was associated with a stronger concentration

of steering values in the lower range, indicating lower observed steering inputs in these cases. A similar trend was observed for ACC, despite being primarily related to longitudinal control rather than steering.

As the observed influence of ACC on SWA was unexpected, a further analysis of cases with activated and deactivated ACC was conducted. The distributions of speed groups for activated versus deactivated ACC are presented in Figure 3.6. Figure 3.6 shows that ACC is more frequently active in higher speed groups, whereas cases without ACC activation are more prevalent across lower speed groups.

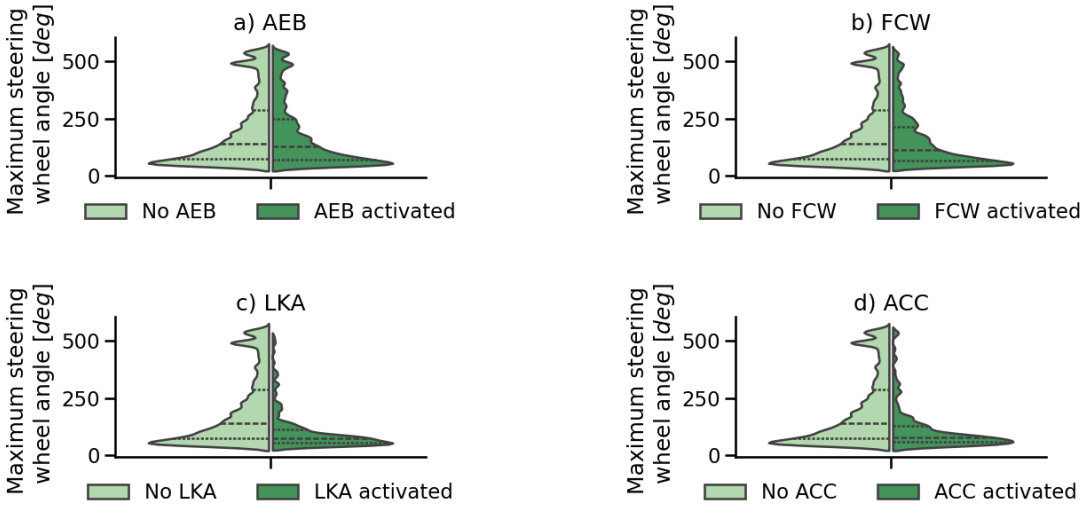

Figure 3.5: Maximum SWA with and without ADAS activation, showing lower steering magnitudes for LKA and ACC and limited differences for AEB and FCW.

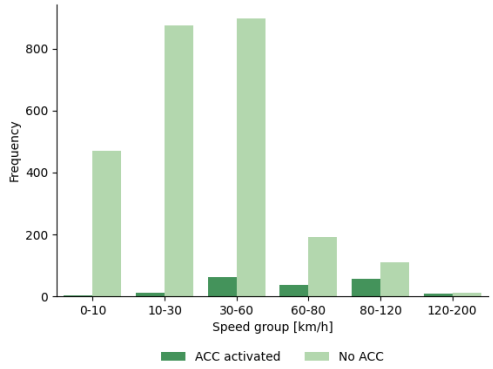

(a) Distribution of speed groups with ACC activated and deactivated, expressed as frequency of occurrence. The total number of cases is 2,558 without ACC activation and 181 with ACC activation.

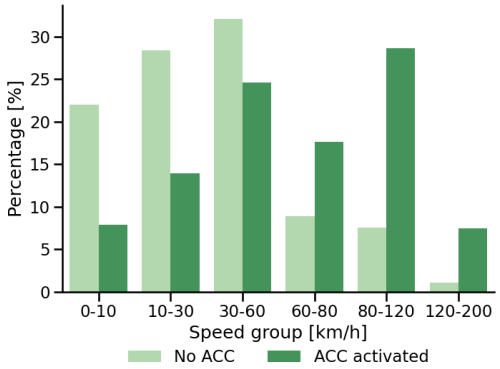

(b) Distribution of speed groups with ACC activated and deactivated, expressed as percentages normalized within each ACC condition. The total number of cases is 2,558 without ACC activation and 181 with ACC activation.

Figure 3.6: Distribution of speed groups for cases without and with ACC.

3.3 Steering wheel angle velocity

The results of the SWAV analyses are presented below, including the estimated maximum driver control limitations for both steering events and evasive steering events.

For SWAV, driving conditions did not have a statistically significant effect. However, a consistent trend was observed in which ADAS activation, regardless of system type, was associated with a slightly lower maximum SWAV, even though the overall distributions did not differ noticeably between ADAS types.

3.3.1 Maximum values and distributions

The distribution of SWAV, excluding values below 3°/s (considered as noise or non-maneuvering), is shown in Figure 3.7 in light red. The distribution is right-skewed, with a high concentration of cases at relatively low steering velocities and a gradual decrease in frequency as steering velocity increases. The 95th percentile is 638°/s.

To isolate characteristic evasive steering behavior, a subset of the data was analyzed using a threshold of SWAV > 300°/s (shown in darker red). Approximately 23.5% of all steering events exceeded this threshold. For this subset, the 95th percentile reaches 858.5°/s, which represents a 95th-percentile estimate of steering velocity during high-urgency maneuvers. This higher percentile value effectively filters out routine steering adjustments and provides a more robust estimate of driver control limitations in crash-imminent situations.

The highest observed maximum value for SWAV was 1300°/s.

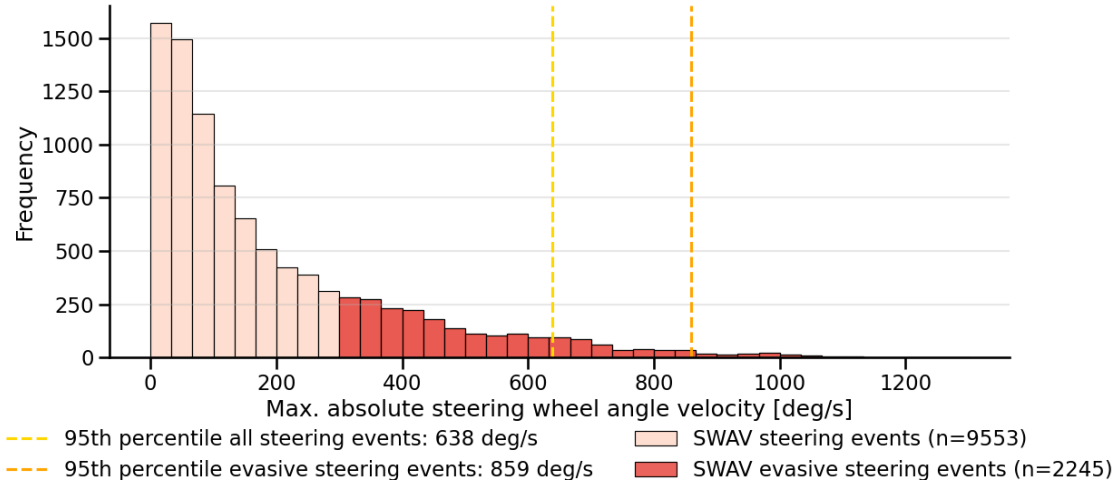

Figure 3.7: Distribution of maximum SWAV for cases above 3.0°/s (light red) and for evasive maneuvers above 300°/s (dark red), including the corresponding 95th percentiles.

The corresponding distributions of vehicle actions and crash types for SWAV values above 3°/s are shown in Figure 3.8a. Driving straight constitutes the largest proportion of cases, while drifting and turning maneuvers represent smaller shares. In terms of crash types, rear-end (strike) collisions dominate, followed by rear-end (struck) and run-off-road events.

For higher steering velocities (SWAV > 300°/s), shown in Figure 3.8b, a clear shift in the distribution is observed, similar to the one observed for the distribution of SWA. The proportion of driving straight decreases substantially, while drifting and turning maneuvers increase. In addition, run-off-road events become more prevalent, whereas both rear-end (strike) and rear-end (struck) collisions decrease in relative frequency.

When examining SWAV across different driving conditions, maximum SWAV did not exhibit statistically significant differences after post-hoc testing.

The largest observed effect size across all comparisons was found for crash type, specifically between SCP and run-off-road events (d = 0.196). Although this effect size represents the largest effect size identified, it still corresponds to a small effect. Figure 3.9 illustrates the similar maximum SWAV distributions across crash types, exemplifying the lack of practical variation in this variable.

Given the absence of meaningful statistical or practical differences in SWAV across different driving conditions, the previously identified 95th-percentile threshold for maximum SWAV (shown in Figure 3.7) can be interpreted as a global maximum SWAV applicable across all driving conditions.

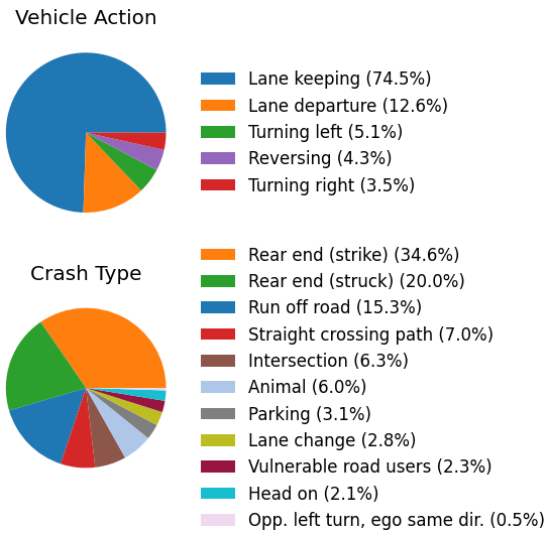

(a) Crash types and vehicle actions for SWAV above 3°/s.

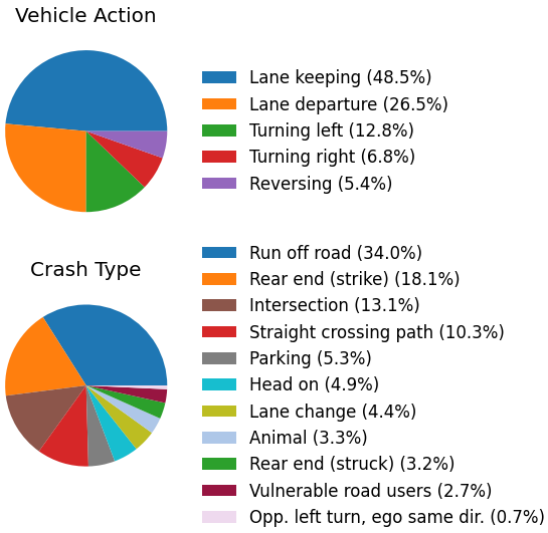

(b) Crash types and vehicle actions for SWAV above 300°/s.

Figure 3.8: Pie charts of the crash types and vehicle actions for normal and evasive SWAV, respectively.

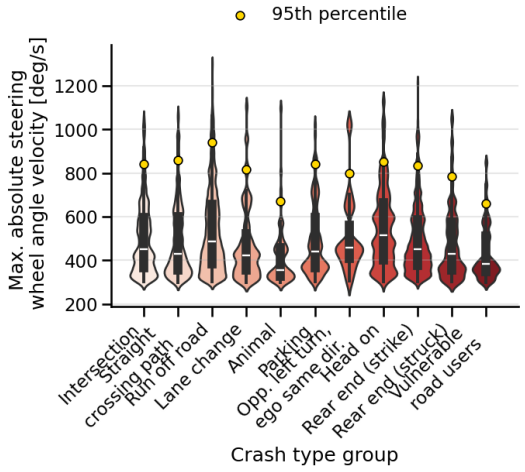

(a) Kernel density distributions (KDE) of maximum SWAV across crash types, estimated using Seaborn's violin plot with an adjusted KDE bandwidth setting (`bw_adjust = 0.3`). Yellow markers indicate the corresponding 95th percentile values, white line markers represent the mean, and black boxes represent the interquartile range with whiskers.

Crash type	Frequency	Mean value	95% percentile	Confidence interval
Intersection	264	501	840	481-521
Straight crossing path	209	490	858	467-513
Run off road	686	540	941	526-555
Lane change	89	471	816	436-516
Animal	66	420	671	385-454
Parking	107	492	841	460-524
Opponent left turn, ego SD	15	507	798	407-607
Head on	99	549	853	512-585
Rear end (strike)	365	496	833	480-513
Rear end (struck)	65	475	783	434-516
Vulnerable road user	55	432	661	398-465

(b) The table summarizes the sample size, mean SWAV, 95th percentile, and confidence interval for each crash type.

Figure 3.9: Relationship between crash types and SWAV.

3.3.2 Advanced driver assistance systems

Figure 3.10 presents a comparison of SWAV across different ADAS. For evasive SWAV ($> 300°/s$), a comparison between cases with and without ADAS activation (64% without activation) shows that the distributions are largely similar regardless of ADAS activation, although slightly lower maximum SWAV values are observed when ADAS are active.

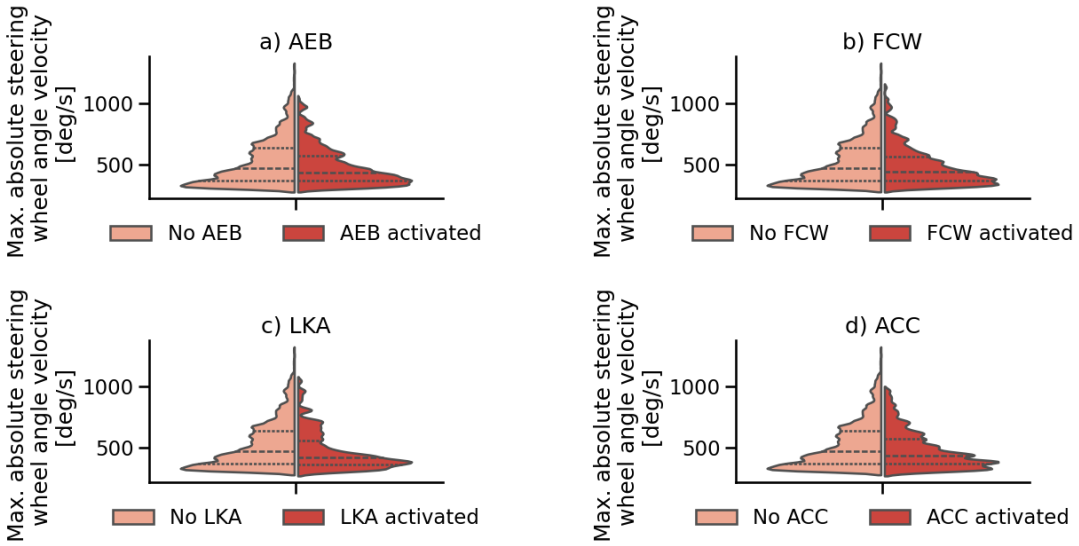

Figure 3.10: Maximum SWAV with and without ADAS activation, showing largely similar distributions across systems, with slightly lower peak values when ADAS are active.

3.4 Driver deceleration request

This section presents the results of the DDR analyses, including the estimated maximum driver control limitations for both braking events and evasive braking events, as well as the influence of different driving conditions. It further provides a more detailed examination of braking patterns derived from DDR, as well as an analysis of the vehicle's actual response to driver braking input.

When analyzing the influence of different driving conditions, both speed groups and vehicle actions each include one category that clearly stands out from the others. In contrast, crash type exhibits three categories that differ from the remaining categories, with medium to large effect sizes. For road conditions, DDR alone was insufficient to capture the effects of reduced friction. Therefore, the actual vehicle deceleration was also examined.

Finally, the results indicate that activation of ADAS, particularly AEB, FCW, and ACC, is associated with drivers reaching maximum deceleration request more frequently compared to cases without ADAS activation.

3.4.1 Maximum values and distributions

Figure 3.11 illustrates the distribution of maximum driver deceleration request, which may include brake system gain, expressed as a percentage of the maximum achievable request. The light blue histogram represents all braking events above 0.5 m/s^2 (threshold for valid braking events), while the dark blue histogram represents evasive braking events above 3.0 m/s^2.

The distribution is heavily skewed towards the upper bound, with a substantial proportion of drivers reaching the maximum deceleration request (100%) prior to the crash. Since DDR is bounded at 100%, the 95th percentile reaches the signal maximum for both braking-event subsets. Within the subset of valid braking events (above 0.50 m/s^2), 58.9% of drivers reach the maximum level. In contrast, 25.8% of all cases do not exhibit braking prior to the crash based on the 0.50 m/s^2 threshold.

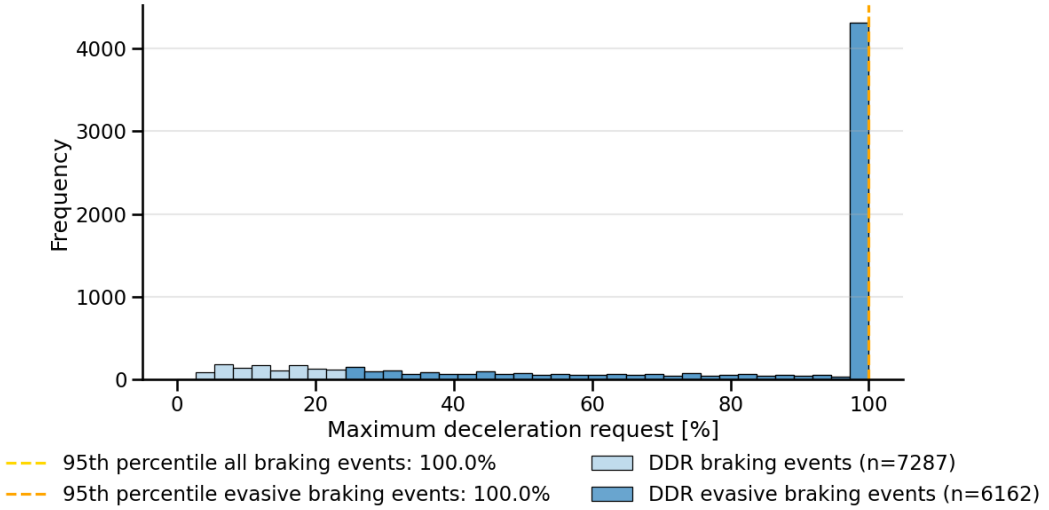

Figure 3.11: Distribution of maximum driver deceleration request (including brake system gain), expressed as a percentage of the maximum achievable request, for normal braking (>0.50 m/s^2) and evasive braking (>3.0 m/s^2), including the corresponding 95th percentiles.

The corresponding distributions of vehicle actions and crash types for DDR values above 0.50 m/s^2 are shown in Figure 3.12a. Driving straight constitutes the largest proportion of cases, while drifting and turning maneuvers represent smaller shares. In terms of crash types, rear-end (strike) collisions dominate, followed by rear-end (struck) and run-off-road events.

For higher-intensity braking (DDR > 3.0 m/s^2), shown in Figure 3.12b, the overall distribution remains largely unchanged. Driving straight continues to dominate among vehicle actions, while drifting and turning maneuvers remain less frequent. Similarly, rear-end (strike) collisions remain the most common crash type, followed by rear-end (struck) and run-off-road events, with only minor variations in relative proportions.

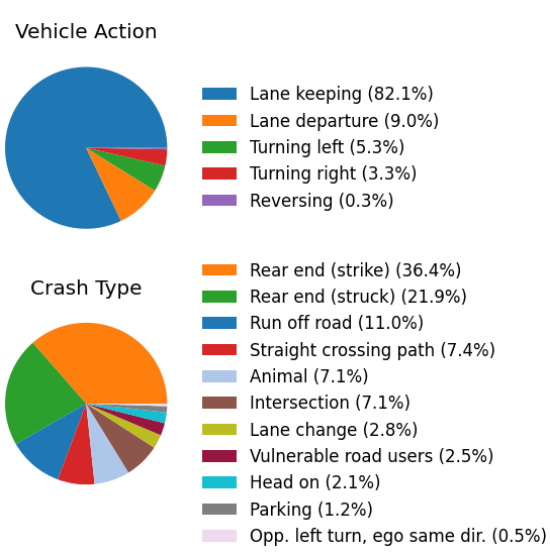

(a) Crash types and vehicle actions for requested deceleration above $0.5m/s^2$.

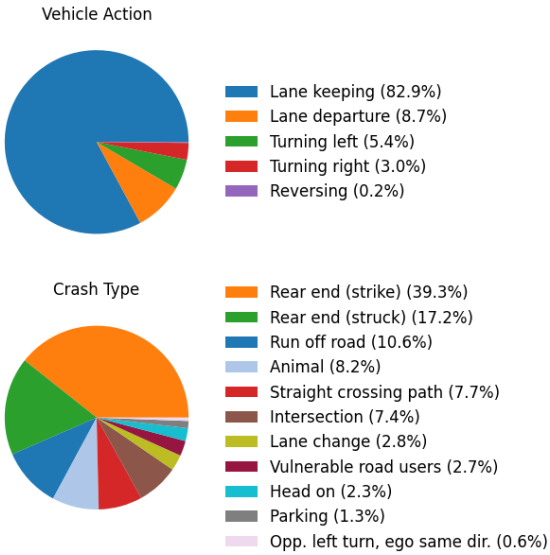

(b) Crash types and vehicle actions for requested deceleration above $3.0m/s^2$.

Figure 3.12: Pie charts of the crash types and vehicle actions for normal and evasive DDR, respectively.

3.4.1.1 Braking pattern

Although the distribution of the DDR shown in Figure 3.11 primarily indicates that most drivers reach the maximum braking request, additional distributions provide further insight into braking behavior. Figure 3.13a presents the distribution of the number of maximum braking requests prior to the crash for all cases, not only braking events. The results show that the majority of drivers either applied maximum braking once (71%) or did not reach maximum braking at all (24%). A small subset of cases involved more than three requests for maximum braking, suggesting a pulsating brake pedal behavior. Approximately 69% of these cases occurred under snowy or icy road conditions, suggesting that road friction may be related to this braking pattern.

Figure 3.13b illustrates the distribution of the duration of maximum braking relative to the total braking sequence. In contrast to the count-based distribution, no clear dominant pattern is observed. Approximately 20% of drivers applied maximum braking for less than 10% of the total braking duration, while the remaining cases are relatively evenly distributed across the full range.

While DDR reflects a driver-related braking request, it does not necessarily represent the resulting physical deceleration of the vehicle. To evaluate how the requested braking translated into actual vehicle deceleration, the distribution of the maximum absolute longitudinal deceleration of the vehicle is presented in Figure 3.14a. As shown, the majority of events occur at relatively low deceleration levels, with a clear concentration in the lower range. The frequency decreases gradually as the deceleration increases. In Figure 3.14b, the distribution of vehicle actions shows that

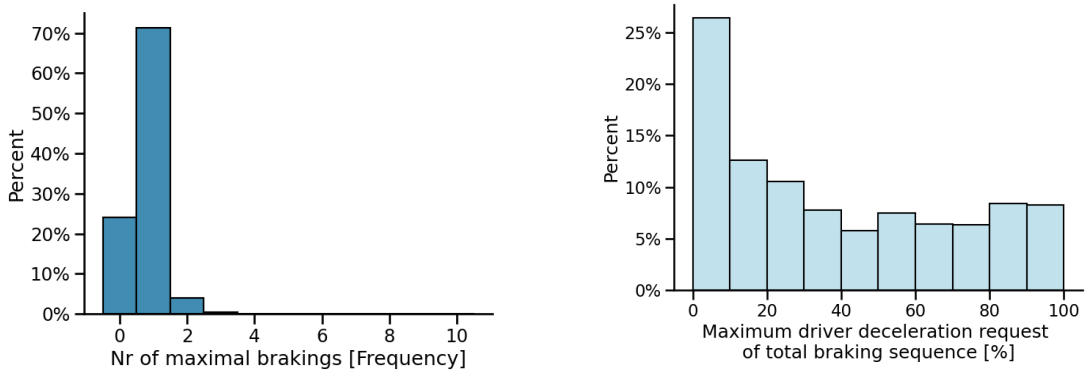

(a) Distribution of the number of maximum deceleration requests prior to the crash, expressed as a percentage of the 9,829 cases.

(b) Distribution of the percentage of the braking sequence spent at maximum braking request, expressed as a percentage of the 9,829 cases.

Figure 3.13: Distributions providing more detailed insight into driver braking behavior prior to the crash. The left plot shows the number of times the driver reaches the maximum deceleration request, while the right plot shows the amount of time for which the maximum deceleration request is reached.

most events occur while the vehicle is driving straight. Other actions, such as drifting out of the lane or turning, represent a smaller proportion of the data. Regarding crash types, rear-end (struck) collisions are the most dominant category, followed by rear-end (strike) and run-off-road crashes. Less frequent categories include side collisions and animal-related incidents.

3.4.2 Speed groups

For deceleration, the speed groups did not exhibit strong statistical differences overall. The only notable difference was observed for the lowest speed group (0-10 km/h), which differed significantly from the higher speed groups between 10 and 120 km/h. This difference was associated with a moderate mean effect (mean d=0.47, range 0.43-0.49), corresponding to larger differences in braking behavior at very low speeds. These results are illustrated in Figure 3.15, which also includes relevant statistical summaries.

3.4.3 Vehicle actions

When examining braking behavior in relation to vehicle action, one category that differs from the others is reversing. This vehicle action exhibits a large average effect size (mean d=1.6, range 1.4-1.7), indicating substantially different braking behavior compared to other vehicle actions. This distinction is illustrated in Figure 3.16, where the driver deceleration request across vehicle actions, together with associated

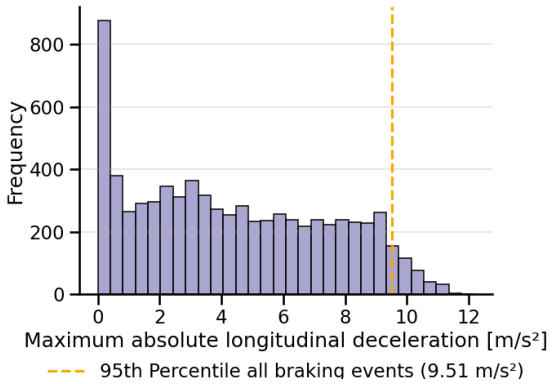

(a) Maximum actual vehicle deceleration distribution.

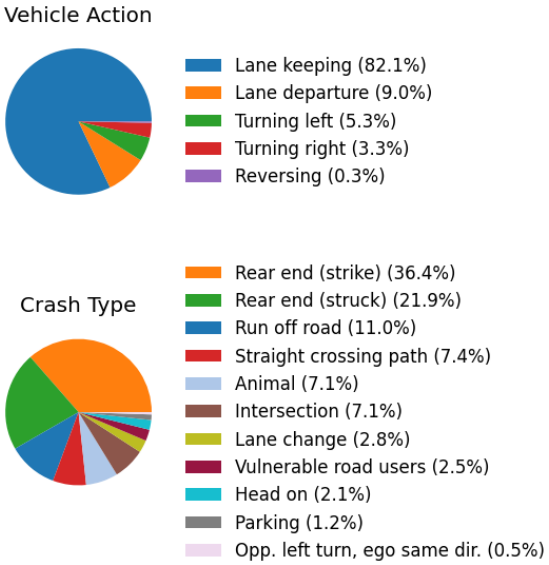

(b) Distribution of vehicle action and crash type.

Figure 3.14: Distributions of actual vehicle deceleration for crashes with driver-requested deceleration above 0.5 m/s^2.

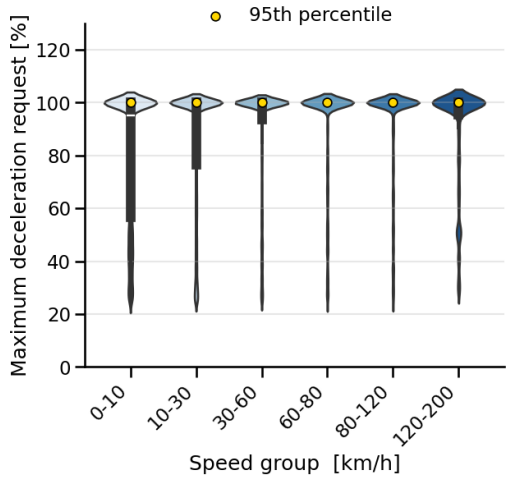

(a) Kernel density distributions (KDE) of maximum DDR across speed groups, estimated using Seaborn's violin plot with an adjusted KDE bandwidth setting (`bw_adjust = 0.3`). Yellow markers indicate the corresponding 95th percentile values, white line markers represent the mean, and black boxes represent the interquartile range with whiskers.

Speed group	Frequency	Mean value	95% percentile	Confidence interval
0-10	1084	83.6%	100%	82.2-85.0%
10-30	971	85.7%	100%	84.0-87.2%
30-60	2049	85.7%	100%	84.6-86.7%
60-80	914	89.0%	100%	87.8-90.6%
80-120	977	89.8%	100%	88.7-91.0%
120-200	167	89.8%	100%	87.0-92.9%

(b) The table summarizes the sample size, mean DDR, 95th percentile, and confidence interval for each speed group.

Figure 3.15: Relationship between speed group and DDR.

statistical summaries, highlights the pronounced separation of reversing from the remaining categories.

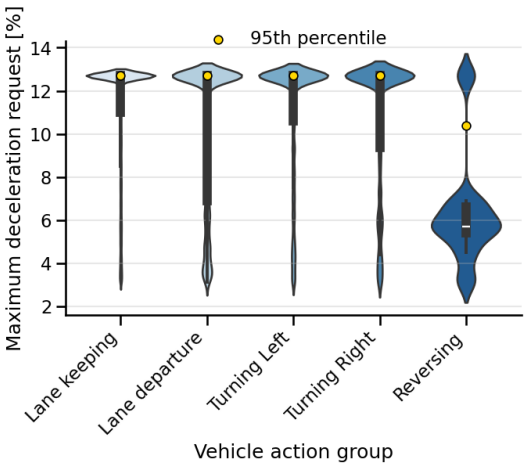

(a) Kernel density distributions (KDE) of maximum DDR across vehicle action groups, estimated using Seaborn's violin plot with an adjusted KDE bandwidth setting (`bw_adjust = 0.3`). Yellow markers indicate the corresponding 95th percentile values, white line markers represent the mean, and black boxes represent the interquartile range with whiskers.

Vehicle action	Frequency	Mean value	95% percentile	Confidence interval
Lane keeping	4938	87.6%	100%	87.0-88.3%
Lane departure	516	78.7%	100%	76.4-81.0%
Turning left	319	86.9%	100%	84.3-89.5%
Turning right	176	84.7%	100%	80.9-88-4%
Reversing	116	49.5%	81.7%	33.3-65.5%

(b) The table summarizes the sample size, mean DDR, 95th percentile, and confidence interval for each vehicle action group.

Figure 3.16: Relationship between vehicle action and DDR.

3.4.4 Crash types

For deceleration, three crash types stood out as markedly different from the majority of the others: *run-off-road, rear-end (struck)* and *parking*. Run-off-road events exhibited a moderate average effect size (mean d=0.56, range 0.25-0.80), while rear-end (struck) crashes showed the largest differences, with a large average effect size (mean d=0.91, range 0.45-1.3). Parking-related crashes also differed from most other crash types, with a moderate average effect size (mean d=0.45, range 0.25-0.72). These differences are clearly visible in the plots shown in Figure 3.17, where these three crash types exhibit noticeably heavier tails compared to the remaining categories.

3.4.5 Road conditions

As previously presented for SWA, road conditions exhibited statistically significant differences for all evaluated variables except DDR. Although no statistically significant differences were observed for DDR after applying the Bonferroni correction, the

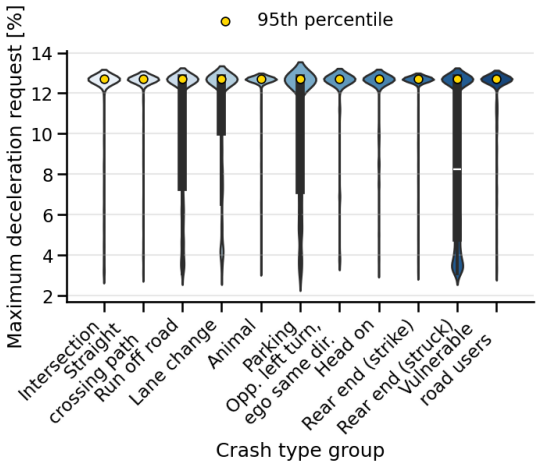

(a) Kernel density distributions (KDE) of maximum DDR across crash types, estimated using Seaborn's violin plot with an adjusted KDE bandwidth setting (`bw_adjust = 0.3`). Yellow markers indicate the corresponding 95th percentile values, white line markers represent the mean, and black boxes represent the interquartile range with whiskers.

Crash type	Frequency	Mean value	95% percentile	Confidence interval
Intersection	439	90.6%	100%	88.6-92.5%
Straight crossing path	458	93.6%	100%	92.0-95.3%
Run off road	631	80.1%	100%	78.0-82.1%
Lane change	166	86.6%	100%	83.0-90.2%
Animal	489	96.0%	100%	94.8-97.2%
Parking	75	81.5%	100%	75.4-87.6%
Opponent left turn, ego SD	35	96.4%	100%	91.6-100%
Head on	135	93.0%	100%	90.0-95.8%
Rear end (strike)	2339	92.3%	100%	91.6-93.1%
Rear end (struck)	1024	66.9%	100%	65.1-68.7%
Vulnerable road user	158	93.9%	100%	91.5-96.4%

(b) The table summarizes the sample size, mean DDR, 95th percentile, and confidence interval for each crash type.

Figure 3.17: Relationship between crash types and DDR.

analysis of actual vehicle deceleration revealed clear effects associated with reduced friction. Specifically, snowy/icy conditions exhibited a medium effect size when compared with both dry (d=0.5) and wet (d=0.6) road conditions. This finding indicates that, although drivers request similar levels of braking across road conditions, the resulting vehicle deceleration differs substantially on low-friction surfaces. This effect for snowy/icy road conditions is illustrated in Figure 3.18, where vehicle deceleration under snowy/icy conditions is noticeably lower compared with wet and dry roads, which exhibit more similar deceleration characteristics.

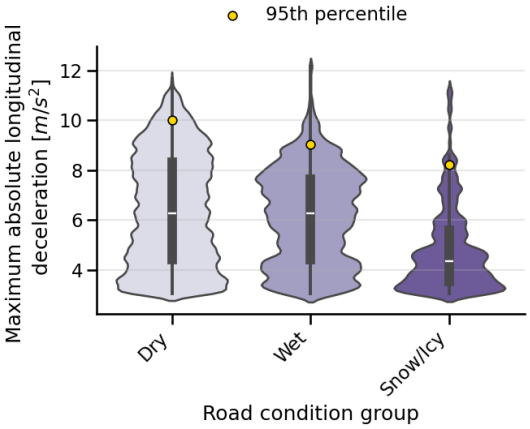

(a) Kernel density distributions (KDE) of actual vehicle deceleration across road conditions, estimated using Seaborn's violin plot with an adjusted KDE bandwidth setting (`bw_adjust = 0.3`). Yellow markers indicate the corresponding 95th percentile values, white line markers represent the mean, and black boxes represent the interquartile range with whiskers.

Road condition	Frequency	Mean value	95% percentile	Confidence interval
Dry	4071	4.83	9.8	4.73-4.93
Wet	616	5.09	8.93	4.89-5.30
Snow/icy	494	3.77	7.52	3.59-3.94

(b) The table summarizes the sample size, mean actual vehicle deceleration, 95th percentile, and confidence interval for each road condition.

Figure 3.18: Relationship between road condition and actual vehicle deceleration.

3.4.6 Advanced driver assistance systems

Figure 3.19 presents a comparison of DDR across different ADAS. For evasive DDR (> 3 m/s^2), a comparison between cases with and without ADAS activation (49% without activation) indicates that a larger proportion of drivers reach maximum deceleration request when ADAS are active. This result is reflected by shifts in the mean and quartile indicators (Q1 and Q3) towards higher values represented by the dashed and dotted lines in Figure 3.19, respectively. This trend is observed across all evaluated ADAS, with the exception of LKA. While LKA still exhibits a slight concentration at lower deceleration request levels, this effect is substantially reduced compared to cases without ADAS activation.

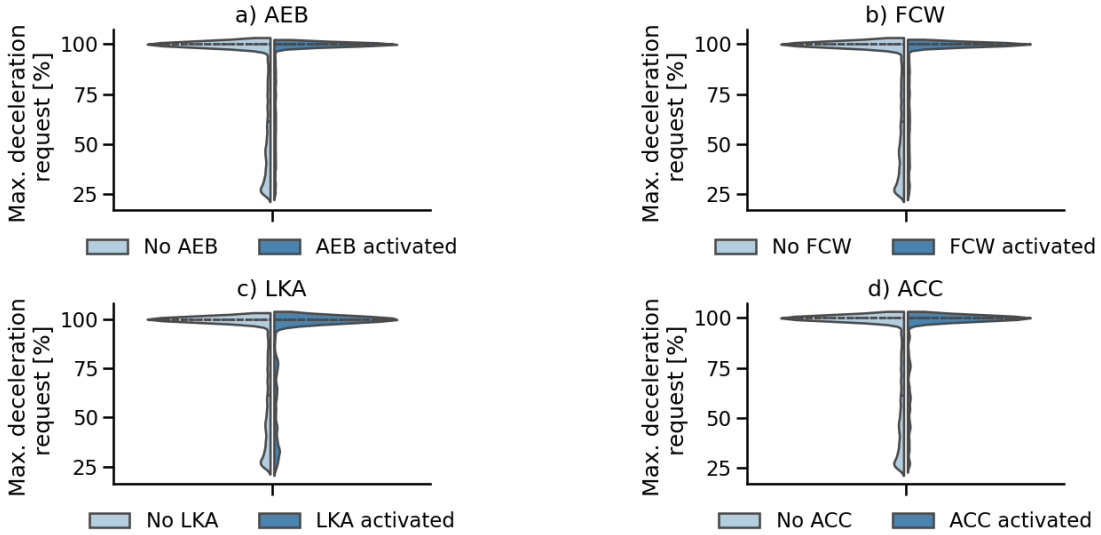

Figure 3.19: Maximum driver deceleration request (DDR) with and without ADAS activation, showing a higher proportion of maximum deceleration request when ADAS are active, with smaller differences for LKA.

3.5 Actual time-to-collision

ATTC reflects the temporal proximity of braking initiation to the crash and is used as a proxy for braking urgency. This section presents the results of the ATTC analyses, including the estimated maximum driver control limitations for both braking events and evasive braking events, as well as the influence of different driving conditions.

When examining the effects of different driving conditions, trends similar to those observed for DDR are identified. Consequently, a more detailed investigation of the crash types run-off-road and rear-end (struck) is presented.

With respect to ADAS activation, no substantial differences in ATTC were observed.

3.5.1 Maximum values and distributions

The distribution of ATTC, defined as the time from the start of the last braking sequence to the crash, is shown in Figure 3.20a. In this analysis, ATTC values are expressed relative to the crash time, where the crash occurs at 0 s. Consequently, more negative ATTC values indicate earlier braking relative to the crash, whereas values closer to 0 s indicate later braking.
The distribution is highly left-skewed, with a large proportion of events occurring close to the time of impact. Approximately 51.4% of the cases exhibit braking onset within 1 second prior to the crash. A smaller number of cases exhibit earlier braking onset, corresponding to more negative ATTC values. The 95th percentile is approximately -0.08 s. A noticeable concentration of cases is observed around -4 s, corresponding to the midpoint of the recorded signal window.

The corresponding distributions of vehicle actions and crash types for these cases are shown in Figure 3.20b. The majority of events occur during straight driving, while turning and lane departure maneuvers represent a smaller proportion of cases. In terms of crash types, rear-end (strike) collisions dominate, followed by run-off-road and rear-end (struck) crashes. To further examine whether the longest ATTC values

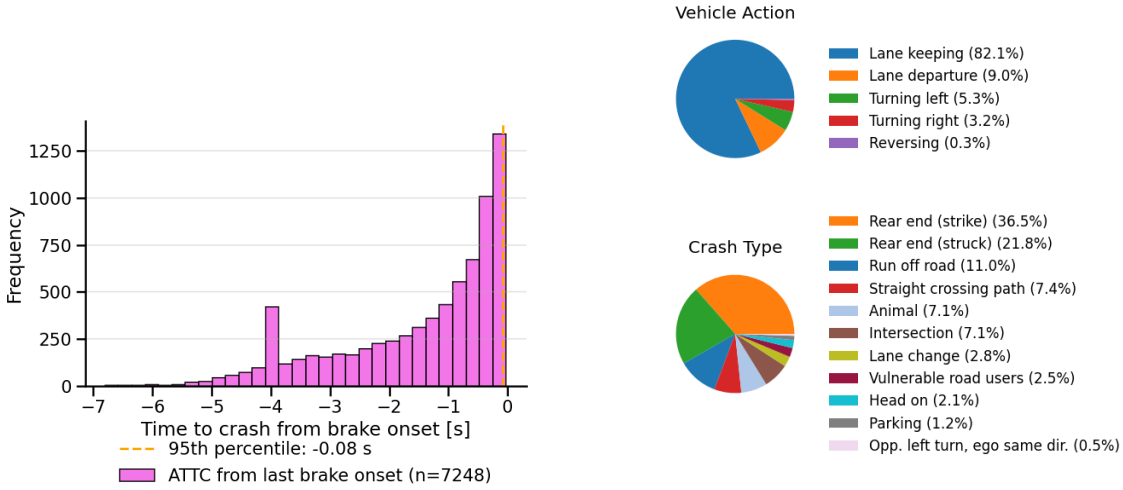

(a) Distribution of ATTC.

(b) Distribution of vehicle action and crash types.

Figure 3.20: Distribution of ATTC and corresponding vehicle action and crash types distributions.

were associated with specific crash types, the ATTC distribution was also stratified by the largest crash-type categories, as shown in Figure 3.21. The stacked histogram shows that rear-end (strike) crashes dominate the distribution overall, particularly for braking onsets closer to the time of impact. However, earlier braking onsets, corresponding to more negative ATTC values, appear to include relatively larger contributions from rear-end (struck) and run-off-road events. A clear concentration is also observed around -4 s, where rear-end (struck) contributes a substantial proportion of the cases. These results indicate that the longest ATTC values are not evenly distributed across crash types, but appear to be associated with a limited number of crash categories.

3.5.2 Speed groups

A similar trend to that observed for DDR was found for ATTC, in which the lowest speed group stood out from the others, although the effect was considerably weaker. The comparison between the lowest speed group (0-10 km/h) and higher speed groups yielded a small mean effect size (mean $d = 0.12$, range 0.04–0.21), indicating only a minor difference in braking timing. No statistically significant differences were found among the higher speed groups.

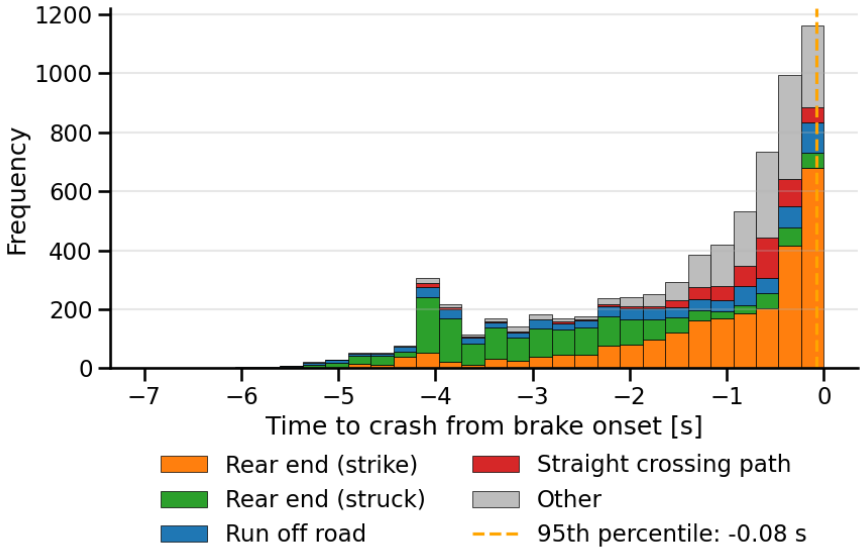

Figure 3.21: ATTC distribution stratified by the major crash types. The stacked histogram shows how the largest crash-type categories contribute across the ATTC range, with the dashed line indicating the 95th percentile at -0.08 s.

3.5.3 Vehicle actions

Similar to the findings for DDR, *reversing* is the vehicle action that is most clearly separated from the others. This distinction is also evident for ATTC, for which reversing exhibits a very large average effect size (d=1.5, range 1.1-2.0). These results further support that reversing maneuvers are associated with substantially different braking behavior compared to other vehicle actions.

3.5.4 Crash types

When crash types are evaluated, a wider range of statistically significant differences is observed across crash types compared with DDR, for which clear differences were limited to three categories. The largest effect sizes for ATTC were found for *rear-end (struck)* crashes (mean d=1.4, range 0.60-1.9), followed by *run-off-road* (mean d=0.73, range 0.51-1.1), *VRU* crashes (mean d=0.69, range 0.32-1.7), *animal* crashes (mean d= 0.87, range 0.31-1.9) and *parking* crashes (mean d= 0.85, range 0.31-1.8).

As illustrated in Figure 3.22, run-off-road and rear-end (struck) crashes are associated with the longest ATTC values, indicating earlier braking relative to the crash. In contrast, VRU, animal, and parking crashes exhibit the shortest ATTC values, indicating later braking relative to the crash. Based on these findings, *run-off-road* and *rear-end (struck)* crashes were selected for further, more detailed investigation, as their ATTC values were most clearly separated from the remaining crash types. A deeper analysis of run-off-road events revealed that these crashes predominantly occur at higher vehicle speeds, as shown in Figure 3.23. Among run-off-road cases

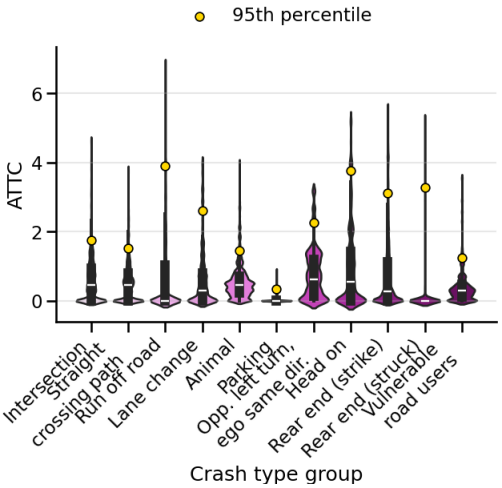

(a) Kernel density distributions (KDE) of ATTC across crash types, estimated using Seaborn's violin plot with an adjusted KDE bandwidth setting (`bw_adjust = 0.3`). Yellow markers indicate the corresponding 95th percentile values, white line markers represent the mean, and black boxes represent the interquartile range with whiskers.

Crash type	Frequency	Mean value	95% percentile	Confidence interval
Intersection	561	-1.09	-0.200	[-1.16, -1.01]
Straight crossing path	619	-0.93	-0.150	[-0.990, -0.860]
Run off road	1364	-1.85	-0.100	[-1.93, -1.77]
Lane change	251	-1.15	-0.150	[-1.28, -1.02]
Animal	537	-0.610	-0.100	[-0.650, -0.560]
Parking	281	-0.320	-0.0250	[-0.380, -0.270]
Opponent left turn, ego SD	44	-0.950	-0.0880	[-1.17, -0.730]
Head on	187	-1.50	-0.100	[-1.68, -1.33]
Rear end (strike)	3211	-1.10	-0.050	[-1.14, -1.06]
Rear end (struck)	1895	-2.74	-0.350	[-2.80, -2.68]
Vulnerable road user	204	-0.63	-0.100	[-0.740, -0.510]

(b) The table summarizes the sample size, mean ATTC, 95th percentile, and confidence interval for each crash type.

Figure 3.22: Relationship between crash types and ATTC.

with earlier braking onset (ATTC < -1.85 s, corresponding to the mean ATTC for this crash type), 81% occurred at speeds exceeding 50 km/h, and 33% of the events took place under snowy or icy road conditions.

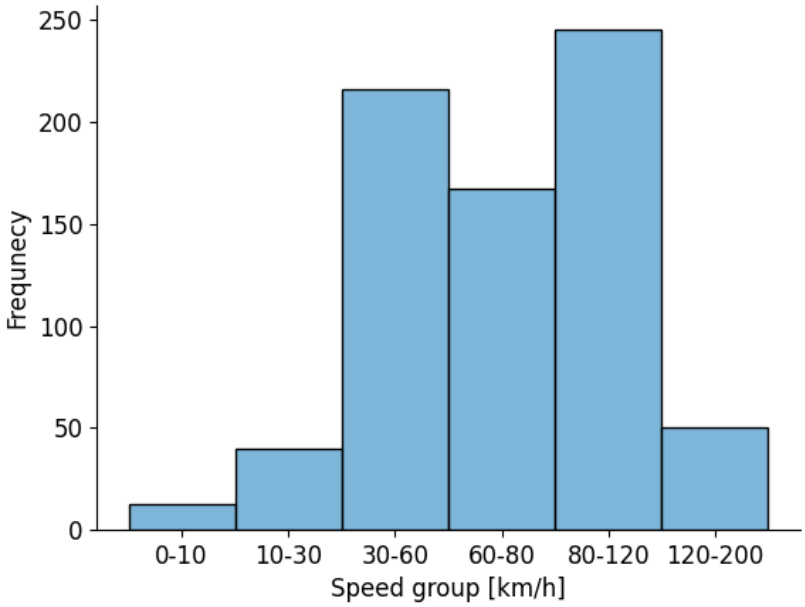

Figure 3.23: Speed distribution of crash type "run-off-road".

Further examination of rear-end (struck) crashes, particularly those with earlier braking onset (ATTC < -2.74 s, corresponding to the mean ATTC for this crash type), indicates that the braking observed in these cases is often not necessarily directly related to the crash itself. Instead, the ego vehicle tends to apply braking in response to a lead vehicle slowing down, after which it is struck from behind by a following vehicle that fails to react in time. This finding suggests that the prolonged ATTC in rear-end (struck) crashes reflects anticipatory braking behavior by the ego vehicle rather than early emergency braking behavior associated with imminent collision.

3.5.5 Road conditions

Similar to the findings for SWA, but with a larger average effect size (mean d=0.36, range 0.30-0.43), ATTC exhibited statistically significant differences for snowy/icy road conditions compared with the other road conditions by showing longer ATTC values.

3.5.6 Advanced driver assistance systems

Figure 3.24 presents a comparison of ATTC across different ADAS. For ATTC, the distributions were similar for cases with and without ADAS activation (48% without

activation), indicating no substantial difference in driver braking timing. However, it should also be noted that cases without ADAS activation may include scenarios with lower urgency, in which braking is initiated earlier despite the absence of assistance. Consequently, the observed similarity in ATTC distributions should be interpreted with caution, as it may reflect differences in situational urgency rather than a lack of ADAS influence alone.

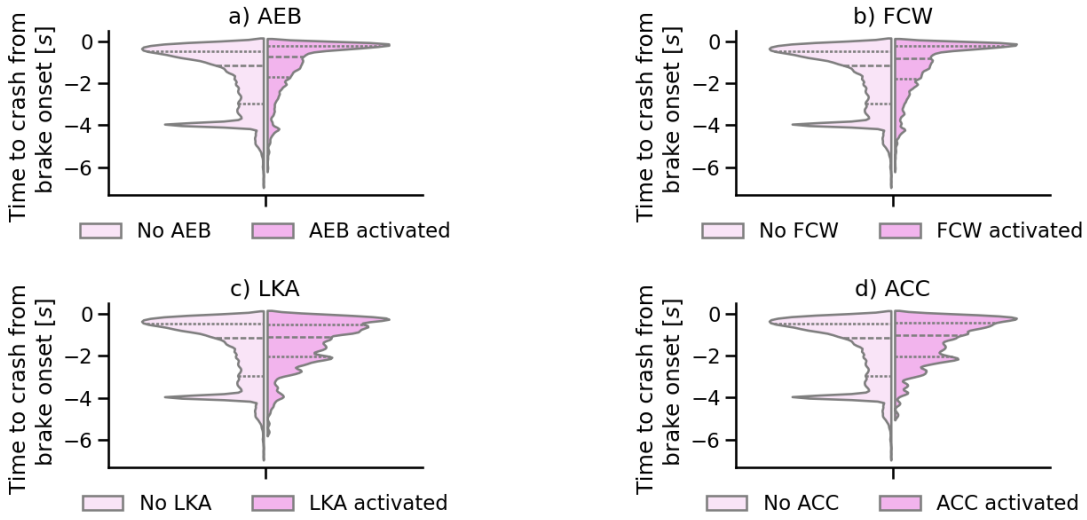

Figure 3.24: ATTC with and without ADAS activation, showing similar distributions across systems and limited influence of ADAS on braking timing.

3.6 Simulation

With the obtained driver control limitations reported in the previous sections and the cut from 3.2s to 6s, resulting in a maneuver of 2.8s, the trajectories shown in Figure 3.25 were obtained and used in the simulation to represent different steering maneuvers.

When incorporating these trajectories into the simulation, all steering maneuvers, except for the case corresponding to SWA/SWAV = 40°/300°/s (representing the lower threshold for evasive maneuvers), successfully avoided the obstacle for both TTC thresholds.
This result is illustrated in Figure 3.26, which presents simulation snapshots for TTC = 1.4 s after the steering maneuver has been initialized. The yellow line represents the trajectory of the ego vehicle (white vehicle). Figure 3.26a shows a case with SWA/SWAV = 40°/300°/s (thresholds for evasive maneuver), where a collision occurs, while Figure 3.26b shows a case with SWA/SWAV = 218°/476°/s (raw data), where the obstacle is successfully avoided.

To further evaluate how close a driver could theoretically approach the obstacle while still being able to avoid a collision, the TTC values were gradually reduced until a

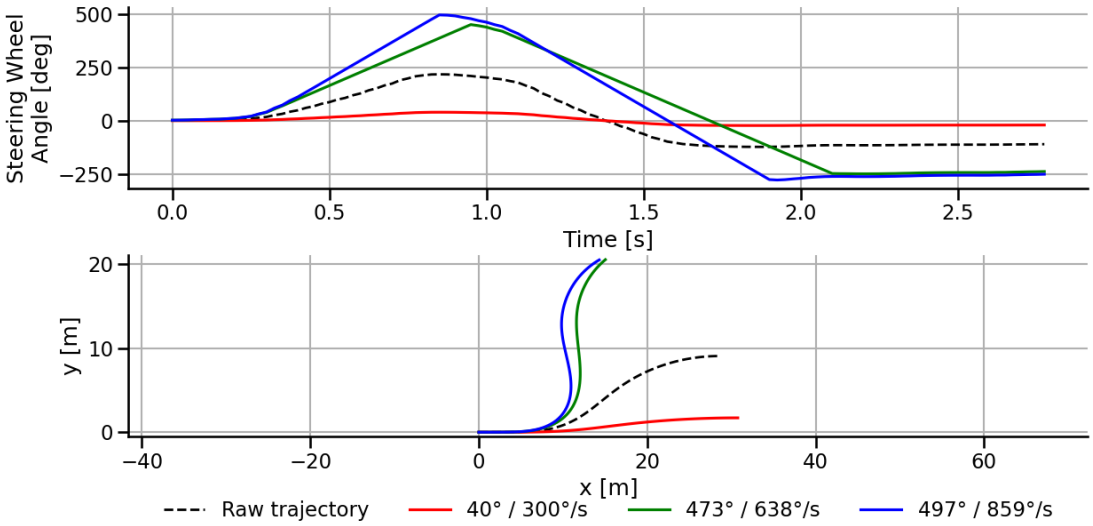

Figure 3.25: Trajectories of SWA and the vehicle trajectory simulated with different limitations on SWA and SWAV.

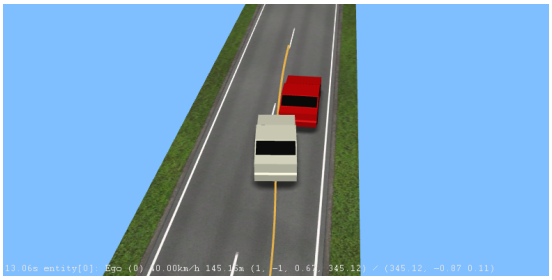

(a) Simulation of a steering maneuver at TTC = 1.4 for SWA/SWAV =40°/300°/s illustrating failure to avoid collision.

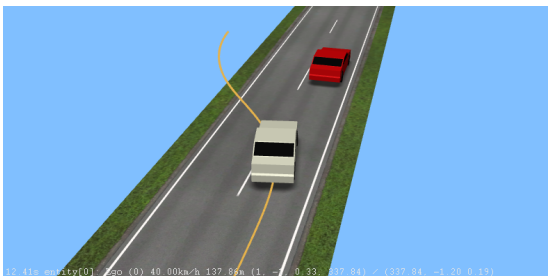

(b) Simulation of a steering maneuver at TTC = 1.4 for SWA/SWAV =218°/476°/s illustrating successful collision avoidance.

Figure 3.26: Simulation of two different steering maneuvers at TTC = 1.4 s.

collision occurred. Using the limits derived from all cases, the shortest TTC at which collision could still be avoided was 0.75 s. When considering only the limits derived from evasive maneuvers, the corresponding threshold was slightly lower, at 0.72 s. These thresholds represent absolute minimum values, implying that the vehicles only avoid collision with a small margin, as illustrated by the example shown in Figure 3.27, where the TTC is set to 0.72 s and the SWA/SWAV= 498°/859°/s.

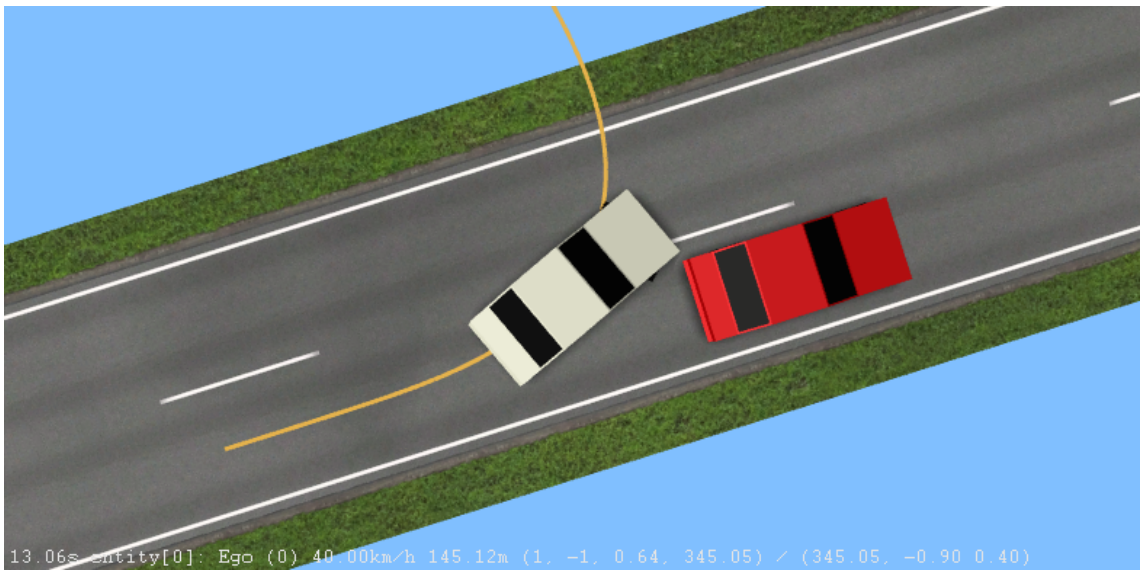

Figure 3.27: Simulation of a steering maneuver at TTC = 0.72 s for SWA/SWAV = 498°/859°/s, illustrating that collision is narrowly avoided.

When conducting the same simulation for AEB, it was observed that the vehicle was able to stop before a collision when a TTC of 1.4 s was applied, for both deceleration levels (-9.27 m/s^2 and -7.19 m/s^2). In contrast, at a TTC of 0.96 s, collisions occurred for both deceleration levels.

The effect of the different TTC thresholds is illustrated in Figure 3.28. Figure 3.28a, corresponding to TTC = 0.96 s, shows that the collision is not avoided, whereas Figure 3.28b, corresponding to TTC = 1.4 s, demonstrates successful collision avoidance.
When the same simulation was conducted with the ego vehicle traveling at 70 km/h, the results showed slight differences: one additional case successfully avoided the obstacle through steering, while one fewer case was able to stop in time using braking alone. A summary of the avoidance outcomes for the different test cases is presented in Table 3.1. In addition, the shortest TTC values obtained without a collision were 0.60 and 0.59 for SWA/SWAV = 473°/638°/s and 497°/859°/s respectively.
An important consideration in these simulations is that applying the 95th-percentile values as maximum steering limits may not be appropriate for rear-end scenarios. When these limits are applied, the resulting trajectories will cause the ego vehicle to leave the roadway, leading to a crash of a different type, such as run-off-road, rather than successfully avoiding a collision.

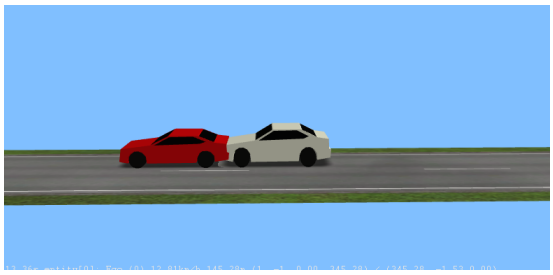

(a) Simulation of AEB activation at TTC = 0.96 s for a deceleration level of -9.27 m/s^2.

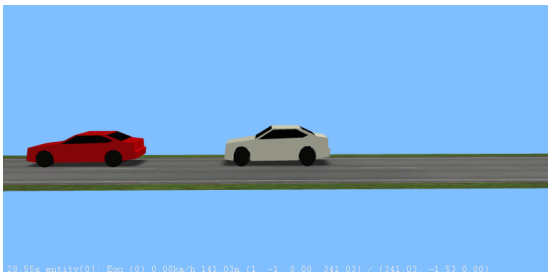

(b) Simulation of AEB activation at TTC = 1.4 s for a deceleration level of -9.27 m/s^2.

Figure 3.28: Simulation of AEB activation at two different TTC values.

	TTC = 0.96 s Speed = 40 km/h	TTC = 1.4 s Speed = 40 km/h	TTC = 0.96 s Speed = 70 km/h	TTC = 1.4 s Speed = 70 km/h
40°/300°/s	No avoidance	No avoidance	No avoidance	Avoidance
218°/476°/s	Avoidance	Avoidance	Avoidance	Avoidance
473°/638°/s	Avoidance	Avoidance	Avoidance	Avoidance
497°/859°/s	Avoidance	Avoidance	Avoidance	Avoidance
-7.19 m/s^2	No avoidance	Avoidance	No avoidance	No avoidance
-9.27 m/s^2	No avoidance	Avoidance	No avoidance	Avoidance

Table 3.1: Summary of avoidance outcomes for different steering and braking scenarios.

This observation is supported by the analysis of run-off-road events. For cases with driving speeds exceeding 40 km/h, the highest SWA was 253°, which is substantially lower than the proposed maximum limits. Despite this lower steering magnitude, the corresponding maximum SWAV reached 859°/s, matching the 95th-percentile value for evasive cases.

4

Discussion

By analyzing steering wheel angle (SWA), steering wheel angle velocity (SWAV), driver deceleration request (DDR), and actual time-to-collision (ATTC), the study aimed to identify representative upper-limit estimates of driver control behavior under different driving conditions and crash scenarios.

The results showed that SWA varied depending on the driving context and crash scenario, particularly across different vehicle actions. In contrast, SWAV remained comparatively stable across different conditions, suggesting that steering rate may represent a more globally constrained aspect of driver behavior. For braking behavior, the results indicated that drivers frequently reached the maximum driver deceleration request level prior to the crash, although the actual longitudinal deceleration of the vehicle remained dependent on environmental factors such as road friction. Furthermore, the ATTC analysis showed that braking is often initiated very late prior to impact, highlighting the importance of ADAS in compensating for delayed human responses in crash-imminent situations.

4.1 Data preprocessing

The preprocessing of the crash database was a critical step for ensuring that the extracted driver control limitations were based on reliable and physically meaningful data. Since the database consists of large-scale real-world crash recordings, several challenges related to signal quality, sensor failures, and annotation accuracy had to be addressed before statistical analysis could be performed. The following sections discuss the implications of the data screening, cleaning, and crash index re-annotation procedures.

4.1.1 Data screening

The data screening process enabled the identification of signals representing steering inputs, such as SWA and SWAV, driver-related braking demand represented by DDR, and contextual variables including crash type, vehicle action, and environmental conditions. This combination made it possible to investigate driver control limitations not only in terms of their magnitude, but also in relation to the driving situations in which they occurred. Consequently, the study provides a more context-dependent understanding of driver behavior compared with analyses based solely on

isolated vehicle dynamics variables.

A particularly important methodological choice was the segmentation of crash sequences into pre-crash and post-crash phases. By excluding post-crash data when identifying maximum driver inputs, the analysis aimed to ensure that the extracted values reflected intentional driver behavior rather than crash-induced sensor artifacts or involuntary vehicle dynamics caused by the impact. Without this separation, the estimated control limits would likely have been unrealistically high. However, the exact transition between pre-crash and post-crash behavior depends strongly on the accuracy of the crash index annotation, introducing uncertainty into the extracted maximum values.

4.1.2 Data filtering

The filtering procedure substantially improved the reliability of the dataset by excluding cases with inconsistent recordings, stationary vehicles, and sensor failures occurring during crash impact. In particular, the removal of extreme steering-related outliers was necessary to avoid overestimating driver control limitations. Inspection of these cases showed that many unrealistic values originated from sensor or transducer failures caused by the crash itself rather than from actual driver inputs.

4.1.3 Re-annotation of crash index

The re-annotation procedure highlighted the challenges associated with determining the exact timing of crash events in real-world data. Since the crash index defines the boundary between pre-crash and post-crash behavior, inaccuracies in this annotation can directly affect the estimated maximum driver inputs. The re-annotation process was therefore an important step for improving the validity of the extracted control limitations.

The inter-rater agreement analysis demonstrated that certain crash types were substantially more difficult to annotate consistently than others. In particular, run-off-road events showed relatively low agreement between annotators. For run-off-road events, a crash index is inherently less well defined than for collision-based crash types. For collisions involving another vehicle or object, the crash index can typically be defined as the first physical contact. In contrast, run-off-road events often represent a gradual transition rather than a single discrete event.

Although several supporting rules were introduced, such as defining the crash index based on two wheels leaving the roadway, visible snow displacement, curb contact, or SWAV peaks, these cues still required subjective interpretation for the run-off-road cases. In particular, snowy conditions and unclear roadway boundaries made it difficult to determine the exact sample at which the vehicle should be considered to have left the roadway, as the crash index often depended on visual interpretation of

cues such as snow displacement or estimated wheel position relative to the roadway. Consequently, even with predefined rules, disagreements within both five and ten samples remained relatively common for this crash type.

Although run-off-road events and cases with missing crash index annotations were associated with the greatest annotation difficulties, the re-annotated cases represented only a limited subset of the full dataset (234 out of 9,829 cases, approximately 2.4%). Of these cases, 65.4% were either classified as run-off-road events or involved missing crash index annotations, as reported in Section 2.2.5. Since the identified annotation uncertainties were concentrated within a relatively small proportion of the full dataset, their influence on the aggregated distributions is expected to be limited. However, the effect may be more pronounced when analyzing specific crash types.

To reduce the subjectivity in these cases, annotation rules were established prior to the re-annotation process, and difficult cases were reviewed jointly by two annotators. Although these measures improved consistency, some degree of subjectivity remains unavoidable when interpreting complex real-world crash scenarios. This limitation affects the reproducibility of the annotations and therefore also the precision of the resulting control limitation estimates.

At the same time, the re-annotation process can be considered a strength of the study, since it reduced the likelihood that unrealistic maximum values originated from incorrectly assigned crash indices. Without this manual verification step, post-crash signal behavior would risk misinterpretation as extreme driver input, leading to an upward bias in the estimated driver control limitations.

4.2 Lighting conditions

The omnibus testing revealed no statistically significant effects of lighting conditions on SWA, SWAV, or ATTC. Although a statistically significant effect was initially observed for DDR, this effect did not remain significant after applying the Bonferroni correction in the post-hoc testing.

These findings contrast with previous work by Oliver et al. (2023), which reported that nighttime driving is associated with shorter available reaction times and consequently more aggressive braking. One possible explanation for this discrepancy is that the study by Oliver et al. (2023) was conducted in a simulation environment and focused exclusively on scenarios involving a stopped or slowed-down lead vehicle. In contrast, the present thesis analyzes a real-world crash database encompassing a wide range of crash types and driving scenarios, which may dilute effects observed under more controlled conditions where the exact same scenario can be re-used and compared.

4.3 Steering wheel angle

The relative maximum SWA was included in the analysis to account for situations where the steering wheel is already biased due to road curvature prior to the critical event. The intention was to reduce the influence of baseline steering and instead capture changes in steering demand associated with potential crash avoidance behavior.

However, the analysis showed that the relative formulation introduces a number of extreme values, where 73% of the highest observed values were associated with parking maneuvers. These scenarios occur at very low vehicle speeds, where rapid steering reversals are observed as the driver transitions between steering directions within a short time interval. Although these cases produce large relative steering values, they do not necessarily reflect crash avoidance behavior, but rather low-speed maneuvering characteristics. As a result, the inclusion of these values leads to an upward bias in the upper percentiles of the distribution.

Having established the normal maximum SWA as the most robust and representative metric, the subsequent analysis focused on its variability under different driving conditions. The speed groups did not exhibit pronounced statistical differences when compared with one another. Although SWA showed statistically significant differences for some of the lower speed groups, the associated effect sizes were small. One plausible explanation for the observed differences is that the speed groups are inherently linked to different road types (e.g., urban, rural, or motorway), as described in Section 2.4.1.1.

At higher speeds, such as those encountered on motorways, road geometry is generally characterized by long, straight segments with limited curvature, which naturally limits the magnitude of steering input for driving. In contrast, the lowest speed group includes driving scenarios such as parking maneuvers and navigation through narrow spaces, which inherently require larger steering angles.

In addition, certain crash types are more prevalent within specific speed groups. This relationship is illustrated in Figure 3.23 as an example, and it was further shown that crash type has a statistically significant influence on SWA for most categories. Consequently, the observed differences between speed groups are likely driven by a combination of these underlying factors, rather than speed alone.

One example of these low-speed cases is *reversing*, which exhibited statistically significant differences compared with all other vehicle action categories. In addition to reversing, *turning left*, and *lane departure* also showed significant differences, whereas no significant difference was observed between *turning right* and lane departure. This asymmetry may be explained by traffic orientation. In right-hand traffic environments, previous studies McLaughlin et al. (2009b) and J.-S. Wang and Knipling (1994) have reported a higher frequency of run-off-road events occurring to the right side of the roadway. Under such conditions, turning-right maneuvers and run-off-road events may exhibit more similar steering characteristics, which could

explain the lack of statistically significant differences in SWA between lane departure and turning right.

Another unexpected result emerged from the comparison of ADAS, where ACC exhibited a distribution very similar to that of LKA, despite ACC being primarily a longitudinal control system rather than a steering-related function. From a functional perspective, this would suggest that ACC should resemble AEB and FCW more closely. In contrast, the result of having LKA activated is not surprising, as LKA operates by assisting or correcting lane-keeping behavior, thereby reducing the need for larger steering inputs. One possible explanation for this result is that ACC helps maintain greater headway to lead vehicles, thereby reducing the need for evasive steering maneuvers. Another potential explanation is that ACC is predominantly activated at higher speeds, particularly during rural road and highway driving, as illustrated in Figure 3.6. As shown previously, these road types are associated with lower SWA. Consequently, this interpretation further supports the conclusion that road type has a significant influence on SWA.

For the SWA evasive steering events, the 95th percentile reaches 498.1°, serving as a representative upper-limit estimate of steering magnitude in the analyzed crash data. This value is substantially higher than those reported in test-track experiments. For instance, "Moose-test" studies reported a mean maximum SWA of 170° and an absolute peak of 335° (Breuer, 2017), while the highest maximum SWA across all cases in this thesis reaches 557°. The discrepancy suggests that while the Moose test represents pre-warned maneuvers conducted in a controlled environment, real-world crash scenarios involve a level of acute urgency and panic that can push driver steering inputs far beyond the limits observed in experimental settings. Furthermore, this difference is attributed to the initial state of the vehicle. In controlled experiments, drivers approach the maneuver from a stable and straight path. In contrast, real-world crash data frequently captures maneuvers initiated from non-neutral positions. Examples of this include steering during an ongoing overtaking maneuver or while navigating a curve. In these cases, any pre-existing steering angle is compounded by the emergency evasive input, which results in a higher total SWA.

Based on the obtained 95th percentile, a review of the cases with SWA values exceeding 500° was performed. The review showed that approximately 66% of those cases were classified as either run-off-road or *"Other"* crash types. In comparison, these categories represented only approximately 22% of the noise-filtered SWA dataset (SWA $> 6°$). This indicates that run-off-road and *"Other"* crash scenarios were substantially overrepresented among the most extreme steering maneuvers. One possible explanation is that run-off-road events may involve aggressive corrective steering inputs during loss-of-control situations, resulting in unusually large steering wheel angles. In addition, the high proportion of *"Other"* cases may reflect complex crash dynamics that are difficult to classify within the predefined crash type categories. Although *"Other"* crash types were excluded from the subsequent crash type distribution analyses, they were retained in this exploratory review of extreme SWA cases due to their strong over-representation among the highest steering values.

4.4 Steering wheel angle velocity

The results show that maximum SWAV exhibits relatively limited variation across different speed groups, vehicle actions, crash types, and road conditions. Although several omnibus tests indicated statistically significant differences, the subsequent post-hoc analyses consistently showed small effect sizes, suggesting that the practical differences in steering velocity between groups are limited. This finding indicates that the distribution of steering velocity is largely stable across driving contexts, particularly in crash-imminent situations.

One important implication of this finding is that SWAV appears to represent a more globally constrained aspect of driver behavior compared with SWA. While SWA varied substantially depending on maneuver type and crash scenario, SWAV remained comparatively stable. This finding is consistent with previous experimental studies suggesting that steering wheel angle velocity is less dependent on vehicle speed and more closely related to the urgency and intensity of the maneuver (Blundell & Harty, 2015; Frydrýn et al., 2025). SWA may be more dependent on the pre-crash driving context, since the steering wheel angle can already be non-zero due to preceding maneuvers such as curve driving, lane changes, or overtaking. As a result, the observed SWA at the time of the crash may reflect the driving situation leading up to the event rather than solely the evasive response itself. In contrast, SWAV represents the rate of change of the steering input and is therefore less influenced by the absolute steering position prior to the crash. This characteristic makes SWAV less sensitive to accumulated steering angle from earlier maneuvers, and more representative of the immediate steering response during the critical pre-crash phase.

When looking at Figure 3.10, it can be observed that SWAV exhibits a slightly lower distribution and reduced maximum values when ADAS is activated compared to cases without ADAS. However, the influence of ADAS on SWAV is less pronounced than its influence on SWA, particularly for LKA. This may be attributed to the fact that SWAV represents the rate of change of steering input and is therefore more directly linked to the driver's immediate control actions during evasive maneuvers. In contrast, LKA primarily modifies the steering target or overall steering magnitude rather than the short-term steering dynamics. Consequently, ADAS and particularly LKA activation has a stronger influence on SWA than on SWAV.

Given the stability of SWAV across different driving contexts, the identified 95th-percentile value for evasive steering maneuvers (858.5°/s) can be interpreted as a representative estimate of the upper limit of driver steering input in crash-imminent situations. This value aligns well with previous experimental research, such as the "Moose-test" studies conducted by Breuer (2017), which reported a mean maximum SWAV of 746°/s. The highest observed maximum SWAV in Breuer (2017) (1335°/s) also corresponds closely with the highest observed maximum in this work (1300°/s) as well as with the upper bound reported by Blundell and Harty (2015) (1200°/s).

However, it is important to distinguish the nature of these data sources; while the Moose-test represents pre-warned maneuvers conducted in a controlled environment where drivers were aware of the upcoming task, the results of this thesis are derived from unprepared, real-world crash scenarios. The fact that the 95th-percentile value in this study exceeds the experimental mean suggests that the urgency of a real collision can push drivers toward their practical steering limits, matching or even surpassing the intensity observed in track tests.

4.5 Driver deceleration request

Before interpreting the DDR results, it is important to reiterate that the available signal does not represent pure brake pedal input. As described in Section 2.3.3, the signal includes brake system gain and should therefore be interpreted as an indirect indicator of driver-related braking demand rather than as a direct measure of the braking effort applied by the driver.

The DDR distribution in Figure 3.11 shows that the signal reaches its maximum available level in 58.9% of the cases. However, this result should be interpreted with caution, as the inclusion of brake system gain may contribute to the high DDR values. The relative contributions of driver input and brake system gain cannot be separated using the available signal. Consequently, the result indicates that high DDR levels are frequently reached, but it does not necessarily imply that drivers apply the maximum possible brake pedal input in the majority of cases.

Similarly to SWA, the fact that only the lowest speed group exhibited statistically significant differences in DDR cannot be explained by vehicle speed alone. An important contributing factor is vehicle action. When examining DDR in relation to vehicle action, reversing clearly stands out from the other categories. This vehicle action is almost exclusively performed at low velocities and is therefore predominantly represented in the lowest speed group. Because reversing maneuvers occur at low speeds, high DDR levels are generally not required to bring the vehicle to a complete stop, which explains the heavier distribution tails in Figure 3.15 and 3.16. Consequently, the observed difference in DDR for the lowest speed group is likely driven by the prevalence of reversing maneuvers rather than by speed itself.

Besides speed groups and vehicle actions, which each exhibited a single distinct category, crash type revealed three categories with heavier tail distributions. Among these, *rear-end (struck)* collisions exhibited the largest differences in DDR compared with most other crash types. One possible explanation for this finding is supported by X. Wang et al. (2016) and Xiong et al. (2019), both of which reported a correlation between deceleration magnitude and increased situational risk. In rear-end (struck) cases, the ego vehicle is struck from behind, providing limited opportunity for the driver to perceive an elevated risk or react prior to impact, as the emerging conflict may not be anticipated. As a result, lower DDR levels may be observed compared with crash scenarios in which evasive braking is feasible.

Beyond rear-end collisions, another crash type among the three distinct categories is *parking*. This category is strongly associated with the vehicle action *reversing* and the lowest speed group. Consequently, the DDR results for parking-related crashes can be interpreted using the same underlying explanation as for reversing maneuvers and low-speed driving scenarios.

Thus far, the analysis has focused on factors influencing DDR itself. Road condition, however, introduces a different mechanism, as its primary effect is observed in the vehicle's actual response rather than in the requested deceleration. The results show no statistically significant differences in DDR across road conditions. However, when examining the actual vehicle deceleration, clear effects associated with reduced friction are observed. This indicates that similar DDR levels are reached across road conditions, while the vehicle response is strongly dependent on surface friction. Previous studies support this interpretation, demonstrating that reduced tire-road friction constrains the achievable vehicle response under braking (Ahrens et al., 2026; Aleksendrić et al., 2012; Pacejka, 2006). Consequently, DDR alone does not fully capture braking effectiveness, as the achievable deceleration is constrained by tire–road interaction on low-friction surfaces. The results may suggest that DDR is more strongly related to the perceived urgency of the situation than to the available friction. However, this interpretation should be made with caution given the inclusion of brake system gain in the DDR signal.

This interpretation is further supported by the braking pattern analysis. Repeated maximum DDR levels are more frequent under snowy or icy conditions. This may indicate that drivers attempt to compensate for an insufficient vehicle response by reapplying or increasing their braking effort. Previous research supports this interpretation, as Gillespie (2021) reported that lower friction levels may lead drivers to apply larger control inputs to achieve similar maneuvers under higher-friction conditions. This pattern may be consistent with a feedback-driven control strategy, in which drivers adjust their braking effort in response to perceived vehicle underperformance caused by reduced friction. However, as previously discussed, the influence of brake system gain prevents the relative contribution of driver input from being determined.

Taken together, these results suggest that braking outcomes in pre-crash situations are not solely determined by driver-related braking demand, but also by the interaction between driver behavior, brake-system response, vehicle dynamics, and environmental limitations. Under low-friction conditions, the DDR signal may reach its maximum available level while the vehicle remains unable to achieve the requested deceleration.

Another observation related to the vehicle's actual deceleration, which is difficult to fully explain, is the absence of a pronounced peak at higher deceleration levels, despite the fact that the DDR signal reaches its maximum available level in the majority of cases. An initial hypothesis was that ATTC is often so short that, although

a high deceleration level is requested, the available time before impact is insufficient for the vehicle to ramp up to higher physical deceleration levels.

However, this explanation is not entirely satisfactory, as a non-negligible number of cases exhibit ATTC values on the order of 3-4 s. From a vehicle dynamics perspective, this duration should be sufficient for the vehicle to achieve substantially higher deceleration levels than those observed. Further investigation is required to disentangle these effects and to better understand the discrepancy between driver deceleration request and the vehicle's actual braking response.

Having discussed limitations related to actual vehicle deceleration, the discussion now shifts back to DDR. Previous analyses of driving conditions identified certain categories associated with lower DDR levels. In contrast, across all evaluated ADAS systems, a higher proportion of cases reached the maximum available DDR level when the systems were activated compared with non-activated cases. This result is accompanied by a general upward shift in the distribution, reflected by increases in both mean and quartile values. However, since the DDR signal includes brake system gain, the observed shift cannot be attributed solely to changes in driver braking effort. It may reflect stronger driver-related braking demand, the influence of brake system gain, differences in scenario criticality, or a combination of these factors. This limitation is particularly relevant when interpreting the results for AEB, FCW, and ACC, as these systems are associated with longitudinal vehicle motion.

In contrast, LKA shows a different pattern. Although a shift towards higher DDR levels is still observed, it is less pronounced than for the other systems. This may be related to the functional purpose of LKA, which primarily supports lane keeping through steering interventions rather than longitudinal vehicle motion. Consequently, LKA has a more limited association with the observed DDR levels.

4.6 Actual time-to-collision

When examining the overall distribution across all crash types, a distinct peak at -4 s can be observed. This peak arises from the automated data-collection trigger, which is activated approximately 4 s prior to the crash. As noted previously, this trigger can be initiated by several system events, such as AEB activation or seatbelt retraction. Consequently, the initiation of emergency braking, corresponding to the start of the ATTC, activates the recording, resulting in an accumulation of observations at this time point and thereby producing the observed peak in the distribution.

Another observation from the overall distribution is that the 95th percentile occurs at -0.08 s prior to the crash. This finding highlights the importance of ADAS implementation and further development. Although drivers reach maximum deceleration request, as indicated by the results of the DDR analyses, these responses occur too late to prevent a collision.

When examining individual crash types, the results obtained for ATTC can be di-

rectly linked to those observed for DDR. The three crash types that stood out for DDR, run-off-road, parking, and rear-end (struck), were characterized by heavier distribution tails, indicating lower deceleration requests. These same crash types also stood out for ATTC, where run-off-road and rear-end (struck) exhibited earlier braking onset, while parking exhibited later braking onset.

Further investigation of run-off-road crashes revealed that these events frequently occur at higher vehicle speeds and predominantly in curved road segments. This finding contrasts with the results reported by McLaughlin et al. (2009b), who found that 56% of run-off-road events occurred on straight roads, followed by curves at 30%.

The observed prevalence of run-off-road events in curves suggests that drivers may enter the curves at excessive speeds and initiate braking relatively early but with insufficient intensity, ultimately resulting in the vehicle leaving the roadway. As indicated by the DDR results, braking is initiated but not forceful enough to prevent the crash. These cases can therefore be interpreted as situations in which drivers overestimate both their own capabilities and those of the vehicle when negotiating curves, failing to adequately adjust speed. In some instances, this behavior could potentially be linked to speed blindness, particularly when drivers exit high-speed motorways onto lower-speed roads featuring curves.

As discussed previously, run-off-road crashes represent a more complex crash type, as they do not necessarily involve a direct collision and the exact moment of the crash can be difficult to determine. This complexity may influence driver behavior, since the perceived urgency of drifting off the roadway may be lower than that associated with an imminent collision with another vehicle. This is particularly relevant given the definition of the crash index for run-off-road events, which is based on the point at which two wheels are assessed to be outside the roadway. This characteristic may also help explain the lower driver deceleration request values observed for run-off-road crashes.

When examining rear-end (struck) crashes, which are associated with the longest ATTC values, the early braking observed should therefore not necessarily be interpreted as a response to the imminent rear-end impact itself. As also indicated by the stratified ATTC distribution in Figure 3.21, these cases may instead reflect an inverse problem, where the primary limitation lies in the response of the following vehicle rather than in the ego vehicle's response or maneuvering. This interpretation also helps explain why the ego vehicle in these events does not reach the same deceleration levels as those observed in other crash types.

Parking is the third crash type for which both DDR and ATTC indicate behavior distinct from the remaining categories. Unlike run-off-road and rear-end (struck) crashes, parking-related crashes are associated with the shortest ATTC values. As discussed in Section 4.4, reversing maneuvers, which predominantly occur at low speeds, are common during parking scenarios. Because these maneuvers occur at

low velocities, drivers generally do not need to apply strong braking, which explains the heavier DDR distribution tails for this crash type. Additionally, ATTC values are short because parking situations characteristically involve very limited margins, leaving little time for reaction.

The remaining crash types with the shortest ATTC values are VRU and animal crashes. These events are defined by sudden and unexpected obstacles entering the roadway. This interpretation is consistent with previous research showing that drivers exhibit longer perception-response times when hazards are unexpected or less anticipated (National Academies of Sciences, Engineering, and Medicine, 2024; X. Wang et al., 2016). Unlike rear-end (strike) crashes, where drivers maintain awareness of a vehicle ahead, VRUs and animals can emerge abruptly from the roadside or from behind other vehicles. As a result, drivers are generally unprepared for these situations, leading to later braking and shorter ATTC.

4.7 Simulation

Based on the simulation results, it can be observed that evasive steering remains feasible even beyond the currently applied thresholds for AEB, provided that drivers apply maximum steering input. This finding suggests that, in certain rear-end (strike) critical situations, current AEB activation strategies may conflict with a driver's intention to avoid a collision through steering alone, even in cases where the driver would otherwise be capable of successfully avoiding the obstacle without system intervention.

This finding further highlights the need for continued development of ADAS, not only with respect to braking but also for steering interventions. The results indicate that sufficiently strong steering inputs in critical rear-end scenarios can enable collision avoidance in situations where AEB, as currently implemented, is unable to prevent a collision.

The results further indicate that once the available TTC is reduced below 0.72 s at 40 km/h and 0.59 s at 70 km/h, drivers no longer have the capability to avoid a rear-end (strike) collision through steering. Consequently, AEB activation should occur no later than at these thresholds.

The difference between using the 95th-percentile steering limits derived from all cases and those derived solely from evasive cases was found to be minimal, with the minimum TTC differing by only 0.03 s at 40 km/h and 0.01 s at 70 km/h. As a result, either threshold can be considered suitable for defining maximum steering capability when applied in this context.

4.8 Limitations and future work

Although this thesis provides representative estimates of upper driver control behavior based on real-world crash data, the results should be interpreted with some caution. The analysis was limited to the signals available in the crash database, such as SWA, SWAV, DDR, and ATTC. These signals provide information about the observed steering and braking behavior, but they do not fully explain why the driver acted in a certain way. For example, the data cannot determine whether the driver detected the hazard late, misjudged the situation, panicked, or intentionally chose a specific maneuver. Therefore, the estimated control limits should not be interpreted as absolute physical limits of human drivers, but rather as observed behavioral limits in the analyzed crash scenarios.

An additional limitation concerns the interpretation of DDR. As discussed previously, this signal does not represent pure brake pedal input, as it also includes brake system gain. Ideally, a raw measure of driver braking input would have been used to characterize driver behavior independently of system-induced amplification. However, such a signal was not available in the dataset. Consequently, further investigation is required to obtain a more precise representation of driver braking behavior and to distinguish between driver input and brake-system response.

Consequently, further investigation of driver braking performance is needed to obtain a more precise representation of driver behavior, particularly in separating pure driver intent from system-induced amplification effects.

A second limitation concerns the absence of driver-specific information. Variables such as age, gender, driving experience, physical capability, risk perception, and familiarity with the vehicle were not available in the dataset. These factors may influence both the magnitude and timing of steering and braking responses. For example, younger and older drivers may differ in reaction time, steering aggressiveness, or braking behavior. Future research should therefore investigate how driver characteristics affect control limitations. This could support the development of more adaptive ADAS thresholds, where intervention strategies are adjusted not only to the traffic situation but also to expected driver response capability.

Another aspect of this thesis that can be viewed as both a limitation and a strength is the use of real-world crash data. A limitation of this approach is that each crash case is unique, meaning that identical scenarios cannot be replicated. As a result, cases grouped under the same driving condition are not entirely comparable, as inherent variability exists within each group. At the same time, this variability constitutes a strength of the study. The inclusion of real-world crash data captures a wide range of driving situations, thereby increasing the likelihood of observing the full extent of driver behavior under critical conditions. Consequently, the estimated driver control limitations provide a more realistic and representative reflection of real-world driving behavior than would be possible using more controlled or synthetic scenarios.

With additional time, the simulation framework could be extended to include a wider range of crash types, road configurations, and vehicle speeds. Such extensions would allow for a more comprehensive evaluation of driver control limitations and could further support the development of ADAS that are better adapted to specific driving situations.

4.9 Implications

The findings of this thesis have several implications for the development of active safety systems and automated vehicles. First, the results show that driver control limitations should not only be described by the maximum magnitude of steering and braking inputs, but also by the timing of these responses and the driving context in which they occur. This is particularly relevant for ADAS functions such as AEB and eLKA, where intervention timing must balance avoiding unnecessary interventions with providing support before the driver's remaining avoidance capability becomes insufficient.

For braking-related interventions, the results show that drivers frequently reach maximum driver deceleration request prior to a crash. However, the ATTC results indicate that braking is often initiated very late, meaning that high braking demand does not necessarily imply sufficient time to avoid a collision. This supports the importance of ADAS systems that can intervene earlier or provide timely warnings when the remaining time margin is too short for the driver to respond effectively.

The proposed maximum driver control limitation for steering can be utilized as a threshold for ADAS activation to intervene when the margin for the driver is too small. Specifically, ADAS could be adjusted to intervene when the driver is unlikely to retain sufficient steering capability to avoid an obstacle independently.

5
Conclusions

This master's thesis investigated driver control limitations and proposed metrics to evaluate them. It also examined how different driving conditions and ADAS activation influence these limitations. The identified control limitations were then implemented in a simulation framework to evaluate current ADAS activation thresholds.

The results demonstrate that steering wheel angle (SWA), steering wheel angle velocity (SWAV), driver deceleration request (DDR), actual-time-to-collision (ATTC), and, in some cases, actual vehicle deceleration are suitable metrics for quantifying driver control limitations.

The driver control limitation values identified in this thesis are based on real-world crash data. For SWAV, these values correspond well with those reported in simulation studies and controlled test-track experiments. This agreement suggests that such experimental studies can reasonably represent real-world driver behavior when assessing SWAV control limits.

Further analysis of the steering metrics SWA and SWAV showed that SWAV is less influenced by driving conditions than SWA. As a result, SWAV can be interpreted as a more robust and context-independent measure of steering control limits. Consequently, SWAV is recommended over SWA when analyzing maximum driver steering control limitations across diverse driving scenarios.

Investigation of the braking metrics DDR and ATTC revealed that drivers consistently reach maximum braking levels, but frequently too late to avoid a collision. This highlights the importance of braking timing, in addition to braking magnitude, when evaluating driver control limitations.

DDR was found to vary only modestly across different driving conditions. However, one distinct category emerged when examining speed groups and vehicle actions. In addition, crash type exhibited statistical differences for parking-related events. Although the initial results indicate that the lowest speed group, the vehicle action *reversing*, and the crash type *parking* differ statistically from other categories, a combined evaluation shows that these cases occur under fundamentally different circumstances compared to the remaining driving conditions. Consequently, vehicle speed cannot be evaluated in isolation; instead, it must be considered in conjunction with driving context, vehicle action, and crash type.

When evaluating the influence of ADAS activation on driver control limitations, a reduced maximum value was observed only for SWAV. This trend may indicate that ADAS activation lowers the perceived urgency of the situations, such that steering maneuvers do not need to be executed as rapidly.

The simulation results indicate that, given the identified driver control limitations, drivers may be capable of steering around an obstacle in a critical rear-end (strike) scenario even beyond the currently applied AEB activation thresholds. This finding highlights that steering can represent a viable and successful avoidance maneuver in situations where braking alone is insufficient to prevent a collision. Consequently, these results suggest that further development of ADAS with respect to steering interventions, either as a complement to or in coordination with braking functions, could be beneficial for improving collision avoidance performance.

Overall, the findings demonstrate that driver control limitations in real-world crashes are shaped not only by the magnitude of driver input, but also by the timing of the response and the surrounding driving context. The proposed metrics and identified control limitation values may therefore provide valuable support for the development and evaluation of future active safety systems and driver models intended to represent realistic human behavior in crash-imminent situations.

6
Ethics and Sustainability aspects

As this thesis is based on the processing and analysis of collected data from real-life crashes, ethical aspects needs to be considered, especially related to GDPR.
The results of this thesis also has the potential of contributing to the improvement of road safety, which in turn can be part of a more sustainable future.

6.1 Ethical aspects

Since the project is partly based on the analysis of an existing crash database, the handling of personal information may be required. For this project, it will primarily involve personal information related to user behavior when analyzing drivers' steering and braking pattern. This type of analysis entails a significant ethical responsibility to ensure that all data are managed in accordance with applicable data protection regulations and ethical guidelines, such as GDPR, and that individual privacy is preserved throughout the project (Integretetsskydds myndigheten, 2025).

To provide the best possible basis for adhering to the guidelines, a GDPR safety training has been completed through Volvo Cars, and the recommended readings from Chalmers have also been reviewed.

This project also has the potential to improve existing vehicle safety functions, such as AEB and eLKA. From an ethical perspective, such improvements may lead to a reduction in traffic accidents and injuries, thereby positively impacting not only vehicle occupants but also other road users.

6.2 Sustainability aspects

This project contributes to social sustainability by addressing road safety, which is a key aspect of sustainable transport systems and can be directly linked to target 11.2 of the United Nations 17 sustainability goals (Nations, 2025). By improving the understanding of human driver control limitations and adapting existing safety systems accordingly, the project has the potential to reduce traffic accidents, injuries, and fatalities.

In addition, improved safety performance can contribute to increased trust in driver assistance and automated driving technologies, supporting a long-term transition

towards safer and more efficient mobility.

Bibliography

Abatan, A., Gupta, N., Jashami, H., Hill, D., Meza, A., Shah, P., Rousch, K., Joshi, N., Yancovitz, C., & Savolainen, P. (2026). Examining the performance of automatic emergency braking systems [AEB TTC 0.96s as average of 17 automakers. Speeds 20/40km/h]. *Transportation Research Record*. https://doi.org/10.1177/03611981251362144

Agnvall, A. (2008). Driving manoeuvre recognition and prediction.

Ahrens, M., Arnold, N., Miller, I., & Siegmund, G. P. (2026, April). *Vehicle deceleration levels during wet-to-dry transitions on an asphalt surface with a high proportion of aggregate* (tech. rep.). WCX SAE World Congress Experience, Detroit, Michigan, United States. https://doi.org/10.4271/2026-01-0542

Aleksendrić, D., Jakovljević, Ž., & Ćirović, V. (2012). Intelligent control of braking process. *Expert Systems with Applications*, *39*, 11758–11765. https://doi.org/10.1016/j.eswa.2012.04.076

Alkim, T. P., Bootsma, G., & Hoogendoorn, S. P. (2007). Field operational test "the assisted driver". *2007 IEEE Intelligent Vehicles Symposium*, 1198–1203. https://doi.org/10.1109/IVS.2007.4290281

Armstrong, R. A. (2014, September). When to use the bonferroni correction. https://doi.org/10.1111/opo.12131

Bachute, M. R., & Subhedar, J. M. (2021). Autonomous driving architectures: Insights of machine learning and deep learning algorithms. *Machine Learning with Applications*, *6*, 100164. https://doi.org/10.1016/j.mlwa.2021.100164

Bellin, M.-Å., Tillgren, P., & Vedung, E. (2012). Vision zero – a road safety policy innovation. *International Journal of Injury Control and Safety Promotion*, *19*(2), 171–179. https://doi.org/10.1080/17457300.2011.635213

Bhattacharyya, R., Brown, K. J., Wang, J., Driggs-Campbell, K., & Kochenderfer, M. J. (2025). A taxonomy and review of algorithms for modeling and predicting human driver behavior. *Proceedings of the IEEE*, 1–23. https://doi.org/10.1109/JPROC.2025.3617487

Blommer, M., Curry, R., Swaminathan, R., Tijerina, L., Talamonti, W., & Kochhar, D. (2017). Driver brake vs. steer response to sudden forward collision scenario in manual and automated driving modes. *Transportation Research Part F: Traffic Psychology and Behaviour*, *45*, 93–101. https://doi.org/10.1016/j.trf.2016.11.006

Blundell, M., & Harty, D. (2015). Active systems. In *The multibody systems approach to vehicle dynamics* (pp. 603–630). Elsevier. https://doi.org/10.1016/b978-0-08-099425-3.00008-x

Breuer, J. J. (2017). Analysis of driver-vehicle-interactions in an evasive manoeuvre-results of ‚moose test" studies.

Brittany N. Campbell, J. D. S., & Najm, W. G. (2003). Examination of crash contributing factors using national crash databases.

Chovan, J. D., Tijerina, L., H, J., Pierowicz, E. (J. A., & (Calspan), D. L. H. (1994). Examination of intersection, left turn across path crashes and potential IVHS countermeasures.

Costa, A. F. D. (2019). Safety impact of advanced driver assistance systems in europe.

D.Bullough, J., Skinner, N., Pysar, R., Radetsky, L., smith, A., & Rea, M. (2008). Nighttime glare and driving performance: Research findings.

de Winkel, K. N., & Christoph, M. (2025). Rethinking advanced driver assistance system taxonomies: A framework and inventory of real-world safety performance. *Transportation Research Interdisciplinary Perspectives*, *29*. https://doi.org/10.1016/j.trip.2025.101336

DeGuzman, C. A., & Donmez, B. (2021). Knowledge of and trust in advanced driver assistance systems. *Accident Analysis and Prevention*, *156*. https://doi.org/10.1016/j.aap.2021.106121

Deligianni, S. P., Quddus, M., Morris, A., Anvuur, A., & Reed, S. (2017). Analyzing and modeling drivers' deceleration behavior from normal driving. *Transportation Research Record*, *2663*, 134–141. https://doi.org/10.3141/2663-17

Deng, J., & Zahabi, M. (2025). Analysis of adaptive systems based on driver's workload. *Applied Ergonomics*, *129*. https://doi.org/10.1016/j.apergo.2025.104585

Dimitriou, L., katerina Stylianou, & b, M. A. A.-A. (2018). Assessing rear-end crash potential in urban locations based on vehicle-by-vehicle interactions, geometric characteristics and operational conditions.

Dinakar, S., & Muttart, J. (2019). Driver behavior in left turn across path from opposite direction crash and near crash events from shrp2 naturalistic driving. *SAE Technical Papers*, *2019-April*. https://doi.org/10.4271/2019-01-0414

Durrani, U., Lee, C., & Shah, D. (2021). Predicting driver reaction time and deceleration: Comparison of perception-reaction thresholds and evidence accumulation framework.

Elvebakk, B. (2007). Vision zero: Remaking road safety.

esmini. (2026). *Environement Simulator Minimalistic (esmini)*. Retrieved May 22, 2026, from https://github.com/esmini/esmini

European Commission. (2021). *Road safety thematic report: Advanced driver assistance systems* (tech. rep.) (Directorate-General for Transport). European Road Safety Observatory. Brussels. Retrieved May 20, 2026, from https://road-safety.transport.ec.europa.eu/document/download/d786ded1-66ce-4571-95e5-1ff38fff5c74_en

Fang, Z., He, J., Qin, P., Chen, H., Zhang, C., & Sun, S. (2025). Enhancing autonomous driving safety in real lane-changing scenarios under friction variability: A friction-adaptive shield reinforcement learning framework. *Accident Analysis and Prevention*, *223*. https://doi.org/10.1016/j.aap.2025.108265

Fitch, G. M., Blanco, M., Morgan, J. F., & Wharton, A. E. (2010). Driver braking performance to surprise and expected events. *3*, 2076–2080. https://doi.org/10.1518/107118110X12829370264529

Frydrýn, M., Kohout, T., Vrtal, P., Svatý, Z., & Nouzovský, L. (2025). Steering wheel angle analysis in evasive maneuvers. *Transportation Research Procedia*, *91*, 790–797. https://doi.org/10.1016/j.trpro.2025.10.101

Gao, J., Yu, B., Chen, Y., Bao, S., Gao, K., & Zhang, L. (2024). An ADAS with better driver satisfaction under rear-end near-crash scenarios: A spatio-temporal graph transformer-based prediction framework of evasive behavior and collision risk. *Transportation Research Part C: Emerging Technologies*, *159*. https://doi.org/10.1016/j.trc.2024.104491

Garrosa, M., Olmeda, E., Del Toro, S. F., & Díaz, V. (2021). Holistic vehicle instrumentation for assessing driver driving styles.

Gillespie, T. D. (2021). Fundamentals of vehicle dynamics.

Harinath, P., Kittane, S. V., Yang, D., Drugge, L., & Jonasson, M. (2020). An adapted evasive manoeuvre assist function for over-reactive and under-reactive drivers. https://doi.org/10.1007/978-3-030-38077-9_118

Hayward, J. C. (1972). Near miss determination through use of a scale of danger.

Heisler, H. (2002). *Advanced vehicle technology* (2nd). Butterworth-Heinemann. https://doi.org/10.1016/B978-0-7506-5131-8.X5000-3

Holocher, S., & Holte, H. (2019, June). Speeding. ESRA2 Thematic report Nr.2. ESRA project (E-survey of Road users' Attitudes).

Integretetsskydds myndigheten. (2025). *Det här gäller enligt dataskydds-förordningen*. Retrieved January 22, 2026, from https://www.imy.se/verksamhet/dataskydd/det-har-galler-enligt-gdpr/

Johansson, Ö., Wanvik, P. O., & Elvik, R. (2009). A new method for assessing the risk of accident associated with darkness. *Östen Johanssona, Per Ole Wanvikb, Rune ElvikAccident Analysis and Prevention*.

Kidd, D. G., Perez-Rapela, D., & Jermakian, J. S. (2023). Characteristics of automatic emergency braking responses in passenger vehicles evaluated in the iihs front crash prevention program. *Accident Analysis and Prevention*, *190*. https://doi.org/10.1016/j.aap.2023.107150

Lee, D. K. (2016). Alternatives to p value: Confidence interval and effect size. *Korean Journal of Anesthesiology*, *69*, 555–562.

Lee, S. E., Llaneras, E., Klauer, S., & Sudweeks, J. (2007). Analyses of rear-end crashes and near-crashes in the 100-car naturalistic driving study to support rear-signaling countermeasure development.

Li, Z., Chen, L., Nie, L., & Yang, S. X. (2022). A novel learning model of driver fatigue features representation for steering wheel angle. *IEEE Transactions on Vehicular Technology*, *71*, 269–281. https://doi.org/10.1109/TVT.2021.3130152

Liu, S.-Y., Engström, J., & Markkula, G. (2025). Automated brake onset detection in naturalistic driving data.

Markkula, G. (2014). Modeling driver control behavior in both routine and near-accident driving. *Proceedings of the Human Factors and Ergonomics Society Annual Meeting*, *58*, 879–883.

Markkula, G. (2015). *Driver behavior models for evaluating automotive active safety from neural dynamics to vehicle dynamics* (tech. rep.). www.chalmers.se

Mazzae, E. N., Barickman, F., Baldwin, G. H. S., & Forkenbrock, G. (1999). *Driver crash avoidance behavior with ABS in an intersection incursion scenario on dry versus wet pavement* (tech. rep.). National Highway Traffic Safety Administration.

Mazzae, E. N., Barickman, F., Forkenbrock, G., & Baldwin, G. H. S. (2003, March). *Test track examination of drivers' collision avoidance behavior using conventional and antilock brakes* (tech. rep.). NHTSA.

McGehee, D. V., Lee, J. D., Rizzo, M., Dawson, J., & Bateman, K. (2004). Quantitative analysis of steering adaptation on a high performance fixed-base driving simulato.

McLaughlin, S. B., Hankey, J. M., Klauer, S. G., & Dingus, T. A. (2009a). Contributing factors to run-off-road crashes and near-crashes.

McLaughlin, S. B., Hankey, J. M., Klauer, S. G., & Dingus, T. A. (2009b, January). *Contributing factors to run-off-road crashes and near-crashes final report* (tech. rep.). www.nhtsa.dot.gov

National Academies of Sciences, Engineering, and Medicine. (2024). *Diagnostic assessment and countermeasure selection: A toolbox for traffic safety practitioners* (J. L. Campbell, L. Hoekstra-Atwood, C. Monk, A. K. Fraser, D. J. Torbic, & I. B. Potts, Eds.). The National Academies Press. https://doi.org/10.17226/27890

Nations, U. (2025). *Goals - 11 - Make cities and human settlements inclusive, safe, resilient and sustainable*. Retrieved January 22, 2026, from https://sdgs.un.org/goals/goal11

Novikov, A., Novikov, I., & Shevtsova, A. (2018). Study of the impact of type and condition of the road surface on parameters of signalized intersection. *36*, 548–555. https://doi.org/10.1016/j.trpro.2018.12.154

Oliver, M., DeLucia, P. R., Jupe, J., Dudley, L., & Weaver, B. W. (2023). Drivers' responses to stopped and slowed lead vehicles during nighttime.

Pacejka, H. B. (2006). *Tire and vehicle dynamics* (2nd ed.). Elsevier Butterworth-Heinemann.

Papazikou, E., Thomas, P., & Quddus, M. (2021). Developing personalised braking and steering thresholds for driver support systems from SHRP2 NDS data. *Accident Analysis and Prevention*, *160*. https://doi.org/10.1016/j.aap.2021.106310

Pawar, N. M., Khanuja, R. K., Choudhary, P., & Velaga, N. R. (2020). Modelling braking behaviour and accident probability of drivers under increasing time pressure conditions. *Accident Analysis and Prevention*, *136*. https://doi.org/10.1016/j.aap.2019.105401

Planek, T. W., Sinelnikov, S., Thomas, J., Kolosh, K., & Porretta, K. (2014). A mathematical model for predicting lane changes using the steering wheel angle. *49*, 1. https://doi.org/10.1016/j.jsr.2014.02.001

SAE International. (2013). Operational definitions of driving performance measures and statistics. (J2944).

Saptoadi, H. (2017). Suitable deceleration rates for environmental friendly city driving. *International Journal of Research in Chemical, Metallurgical and Civil Engineerin*.

Sarkar, A., Hickman, J. S., b, A. D. M., Huang, W., Vogelpohl, T., & f, G. M. (2021). Steering or braking avoidance response in SHRP2 rear-end crashes and near-crashes: A decision tree approach.

Sen, B., Smith, J. D., & Najm, W. G. (2003, March). *Analysis of lane change crashes* (tech. rep.).

Sullivan, G. M., & Feinn, R. (2013). Using effect size—or why the P value is not enough. *Journal of Graduate Medical Education*, *4*, 279–282. https://doi.org/10.4300/jgme-d-12-00156.1

Trafikverket. (2011, November). *Gångtrafiken i samhällsplaneringen*. https://bransch.trafikverket.se/for-dig-i-branschen/Planera-och-utreda/samhallsplanering/planera-for-transporter-i-samhallsplaneringen/Personresor/Gangtrafiken-i-samhallsplaneringen/

Trafikverket. (2022). Nollvisionen är vår ledstjärna. Retrieved May 20, 2026, from https://www.trafikverket.se/om-oss/vi-gor-sverige-narmare/nollvisionen-ar-var-ledstjarna/

Trafikverket. (2024). *Nollvisionen – tillsammans räddar vi liv*. Retrieved January 22, 2026, from https://bransch.trafikverket.se/for-dig-i-branschen/samarbete-med-branschen/Samarbeten-for-trafiksakerhet/tillsammans-for-nollvisionen/

Trafikverket. (2025, December). *Hastighetgränser på väg*. https://www.trafikverket.se/resa-och-trafik/trafiksakerhet/sakerhet-pa-vag/hastighetsgranser-pa-vag/

Uddin, M. G., Rahman, A., Taghikhah, F. R., & Olbert, A. I. (2024). Data-driven evolution of water quality models: An in-depth investigation of innovative outlier detection approaches- A case study of irish water quality index (IEWQI) model. *Water Research*, *255*. https://doi.org/10.1016/j.watres.2024.121499

Union, E. (2024, September). *Road rules and safety - Sweden*. https://europa.eu/youreurope/citizens/travel/driving-abroad/road-rules-and-safety/sweden/index_en.htm#speed_limits

Uttley, J., & Fotios, S. (2017). The effect of ambient light condition on road traffic collisions involving pedestrians on pedestrian crossings.

Varotto, S. F., Jansen, R., Bijleveld, F., & van Nes, N. (2021). Adaptations in driver deceleration behaviour with automatic incident detection: A naturalistic driving study. *Transportation Research Part F: Traffic Psychology and Behaviour*, *78*, 164–179. https://doi.org/10.1016/j.trf.2021.02.011

Vogel, K. (2003). *A comparison of headway and time to collision as safety indicators* (tech. rep.).

Wang, J.-S., & Knipling, R. (1994, March). *Single vehicle roadway departure crashes: Problem size assessment and statistical description* (tech. rep.).

Wang, X., Zhu, M., Chen, M., & Tremont, P. (2016). Drivers' rear end collision avoidance behaviors under different levels of situational urgency. *Transportation Research Part C: Emerging Technologies*, *71*, 419–433. https://doi.org/10.1016/j.trc.2016.08.014

Winner, H., Hakuli, S., Lotz, F., & Singer, C. (2016). Handbook of driver assistance systems.

Wu, K.-F., & Lin, Y.-J. (2019). Exploring the effects of critical driving situations on driver perception time (pt) using shrp2 naturalistic driving study data. *Accident Analysis Prevention*, *128*, 94–102. https://doi.org/https://doi.org/10.1016/j.aap.2019.04.003

Xiong, X., Wang, M., Cai, Y., Chen, L., Farah, H., & Hagenzieker, M. (2019). A forward collision avoidance algorithm based on driver braking behavior. *Accident Analysis and Prevention*, *129*, 30–43. https://doi.org/10.1016/j.aap.2019.05.004

Xue, Q., Markkula, G., Yan, X., & Merat, N. (2018). Using perceptual cues for brake response to a lead vehicle: Comparing threshold and accumulator models of visual looming. *Accident Analysis and Prevention*, *118*, 114–124. https://doi.org/10.1016/j.aap.2018.06.006

Yan, Y., Du, C., Wang, W., Ma, R., Wang, Y., Wang, H., Pi, D., Chen, Y.-H., & Chen, Y. .-. (2025). Road surface status recognition and estimation: State-of-the-art review and research perspectives. *Chinese Journal of Mechanical Engineering*. https://doi.org/10.1016/j.cjme.2025.100170

Zhao, Y., & Lin, Y. (2026a). Why do drivers brake later than AEB in rear-end collisions? An analysis based on drive recorder videos.

Zhao, Y., & Lin, Y. (2026b). Why do drivers brake later than aeb in rear-end collisions? an analysis based on drive recorder videos [TTC for ADAS]. *Accident Analysis and Prevention*, *225*. https://doi.org/10.1016/j.aap.2025.108275

DEPARTMENT MECHANICS AND MARITIME SCIENCES
CHALMERS UNIVERSITY OF TECHNOLOGY
Gothenburg, Sweden
www.chalmers.se

CHALMERS
UNIVERSITY OF TECHNOLOGY